

# Identification of *myo*-Inositol-3-phosphate Synthase Isoforms CHARACTERIZATION, EXPRESSION, AND PUTATIVE ROLE OF A 16-kDa $\gamma_c$ ISOFORM\*

Received for publication, January 12, 2009 Published, JBC Papers in Press, February 2, 2009, DOI 10.1074/jbc.M900206200

Ratnam S. Seelan<sup>‡§1</sup>, Jaganathan Lakshmanan<sup>‡§</sup>, Manuel F. Casanova<sup>‡</sup>, and Ranga N. Parthasarathy<sup>‡§¶1</sup>From the Departments of <sup>‡</sup>Psychiatry and Behavioral Sciences and <sup>¶</sup>Biochemistry and Molecular Biology, University of Louisville, Louisville, Kentucky 40202 and the <sup>§</sup>Molecular Neuroscience and Bioinformatics Laboratories, Mental Health, Behavioral Science, and Research Services, Veterans Affairs Medical Center, Louisville, Kentucky 40206

*myo*-Inositol is an important constituent of membrane phospholipids and is a precursor for the phosphoinositide signaling pathway. It is synthesized from glucose 6-phosphate by *myo*-inositol-3-phosphate synthase (IP synthase), a homotrimer composed of a 68-kDa polypeptide in most mammalian tissues. It is a putative target for mood-stabilizing drugs such as lithium and valproate. Here, we show that the rat gene (*Isyna1*) encoding this enzyme generates a number of alternatively spliced transcripts in addition to the fully spliced form that encodes the 68-kDa subunit (the  $\alpha$  isoform). Specifically, we identify a small 16-kDa subunit (the  $\gamma_c$  isoform) derived by an intron retention mechanism and provide evidence for its existence in rat tissues. The  $\gamma_c$  isoform is highly conserved in mammals, but it lacks the catalytic domain while retaining the NAD<sup>+</sup> binding domain. Both  $\alpha$  and  $\gamma_c$  isoforms are predominantly expressed in many rat tissues and display apparent stoichiometry in purified enzyme preparations. An IP synthase polyclonal antibody not only detects the  $\alpha$  and  $\gamma_c$  isoforms but also several other isoforms in pancreas, intestine, and testis suggesting that the holoenzyme is composed of unique subunits in various tissues. Interestingly, the  $\alpha$  isoform is not expressed in the intestine. IP synthase activity assays using purified  $\alpha$  and  $\gamma_c$  isoforms indicate that the latter negatively modulates  $\alpha$  isoform activity, possibly by competing for NAD<sup>+</sup> molecules. Our findings have important ramifications for understanding the mood stabilization process and suggest that inositol biosynthesis is a highly regulated and dynamic process.

Inositol, a ubiquitous six-carbon cyclic sugar, exists in several stereoisomeric forms, of which the most active physiological form is *myo*-inositol (hereafter, inositol) (1). It constitutes a critical component of membrane phospholipids, mediates osmoregulation, and is an important precursor for the phos-

phoinositide (PI)<sup>2</sup> signaling pathway. It can be phosphorylated at one or more positions in the inositol ring yielding an array of inositol phosphates (IPs) and PIs (2). IPs, ranging from IP<sub>1</sub> to IP<sub>8</sub>, participate in a multitude of key biochemical processes (2): they act as critical second messengers in signal transduction pathways (3), mediate phosphorylation of target proteins (4), participate in chromatin remodeling and gene expression (5–7), facilitate mRNA export from the nucleus (8), etc. The biosynthesis of IPs and PIs (inositol phospholipids) ultimately depends on the availability of free inositol. Tissues obtain inositol through one or more of the following mechanisms: (i) PI turnover through receptor recycling, which generates free inositol from the breakdown of poly-phosphorylated forms; (ii) inositol transport via H<sup>+</sup> or Na<sup>+</sup>/*myo*-inositol transporters; and, (iii) *de novo* synthesis of inositol from glucose 6-phosphate (G6P) via *myo*-Inositol 3-phosphate synthase (hereafter, IP synthase). The brain primarily obtains its inositol through PI turnover and *de novo* synthesis (9, 10).

The brain manifests very high levels of inositol, almost 100 times higher than in blood and other tissues (11, 12). The elevated levels may, in part, be due to its active involvement in the PI signaling pathway, which couples the G-protein activation of numerous receptor systems to the generation of diacylglycerol and IP<sub>3</sub>, two important second messengers, involved in protein kinase C activation and calcium mobilization, respectively (13–15). Profound alterations in brain inositol levels can, therefore, affect brain signaling events leading to severe psychiatric and neurological problems. Altered inositol levels have been observed in the brains of Alzheimer (16, 17) and autism spectrum disorder patients (18) and in suicide (19) and stroke (20, 21) victims. High fetal inositol concentrations in the cerebrospinal fluid have been attributed to the pathogenesis of Down syndrome (22, 23), whereas a deficiency can cause neural tube defects in rat embryos (24). Oral administration of inositol has been found to be therapeutic for obsessive compulsive disorder (25, 26) and panic disorder (27), and inositol intake can reverse brain cell shrinkage in osmotic demyelination syndrome (28). Inositol is known to reduce anxiety-like behavior in mouse models of psychiatric disorders (29). Bipolar patients in the manic phase are often treated with lithium or valproate, two commonly used drugs that decrease free inositol levels by

\* This work was supported, in whole or in part, by National Institutes of Health Grant 5P20RR017702 from the COBRE program of the National Center for Research Resources (NCR), a component of NIH (to R. S. S.). This work was also supported by NIH Grant MH69991 (to M. F. C.) and by the Office of Research and Development, Medical Research Service, Dept. of Veterans Affairs, Washington, D. C. (to R. N. P.). The contents of this publication are solely the responsibility of the authors and do not necessarily represent the official views of NCR or NIH. Human brain tissues were provided by the Harvard Brain Tissue Resource Center, which is supported in part by NIH Grant R24MH068855.

<sup>1</sup> To whom correspondence should be addressed: Dept. of Molecular, Cellular, and Craniofacial Biology, Birth Defects Center, 501 S. Preston St., University of Louisville, KY 40202. Tel.: 502-852-1843; Fax: 502-852-4702; E-mail: rsseel01@louisville.edu.

<sup>2</sup> The abbreviations used are: PI, phosphoinositide; G6P, glucose 6-phosphate; HEK, human embryonic kidney; IP, inositol phosphate; IP<sub>1</sub>, inositol monophosphate; IR, intron retention; MALDI-TOF, matrix-assisted laser desorption/ionization-time of flight; MS, mass spectrometry; ORF, open reading frame; nt, nucleotide(s).

## myo-Inositol-3-phosphate Synthase Isoforms

inhibiting inositol monophosphatase 1 and IP synthase, respectively (9), whereas oral administration of inositol can alleviate the depressive phase of bipolar disorder (30). Not surprisingly, IP synthase is considered to be a potential drug target for mood stabilization (31, 32).

IP synthase (EC 5.5.1.4) is a rate-limiting enzyme that catalyzes the first step in the biosynthesis of all inositol containing compounds (33). It converts G6P to *myo*-inositol 3-phosphate (IP<sub>1</sub>) via a three-step reaction: (i) oxidation of G6P to 5-keto G6P by NAD<sup>+</sup>, (ii) intramolecular aldol cyclization to form inosose 2,1-phosphate, and (iii) its reduction to IP<sub>1</sub> by NADH. The phosphate moiety in IP<sub>1</sub> is subsequently removed by inositol monophosphatase 1 to produce free inositol. The mechanism of enzyme action was first demonstrated in the 1960s by groups led by Eisenberg, Loewus, and Hoffmann-Ostenhof (34–37).

Mammalian IP synthase was first purified by Maeda and Eisenberg from rat testes (38), the principal tissue of mammalian inositol biosynthesis and the richest source of this enzyme. It is present in diverse organisms ranging from prokaryotes (cyanobacteria, eubacteria, and archaea) to eukaryotes (fungi, plants, and animals) (39). The native enzyme is typically a homotrimer made up of ~68-kDa subunits in mammalian cells and a homotetramer in yeast and plant cells. Crystallographic studies indicate that the protein is made up of three domains (40, 41): (i) a “central domain” comprising the N and C termini, which make the majority of contacts between monomers, (ii) an “NAD-binding domain,” and (iii) a “catalytic domain” that binds the substrate, G6P. The rat enzyme is encoded by the *Isyna1* gene, which consists of 11 exons and 10 introns. Human *ISYNA1* encodes an mRNA of ~1.8 kb that is expressed variably in different tissues (42) with the highest expression in testis followed by heart, placenta, kidney, and pancreas; intriguingly, brain manifests low expression; almost no expression is observed in peripheral blood leukocytes, colon, and thymus (42). *ISYNA1* is located in 19p13.1, a susceptibility locus for autism spectrum disorders (43).

Yeast IP synthase encoded by the *INO1* gene has been extensively studied and well characterized (44, 45). *INO1* expression is repressed in the presence of inositol and derepressed in its absence (46–48). Studies in yeast indicate that lithium and valproate deplete intracellular inositol levels, thereby derepressing *INO1* expression. These drugs appear to act by different mechanisms: lithium inhibits inositol monophosphatase 1 preventing IP<sub>1</sub> conversion to inositol, whereas valproate inhibits IP synthase resulting in decreased IP<sub>1</sub>, and therefore to decreased inositol, levels (9, 49). The therapeutic efficacy of lithium in treating bipolar disorder is attributed to its ability to decrease inositol levels and forms the basis for the “inositol depletion hypothesis” (12, 50), a theory that has been challenged by others (51).

Very little is known about the regulation of mammalian IP synthase. Enzyme activity in testis is found to be decreased in rats subjected to long term diabetes (52). Decreases in activity have been observed in the reproductive organs and liver of hypophysectomized male rats and in the liver of thyroidectomized male rats (53), whereas estrogen has been found to induce this enzyme in rat uterus (54), suggesting hormonal reg-

ulation of IP synthase expression. Hasegawa and Eisenberg (53) conclude that IP synthase in male reproductive organs is under the direct control of the pituitary, whereas in the liver it is mediated by the thyroid. IP synthase activity is also increased in the mammary glands beginning at parturition (55). Rats treated chronically (10 days) with therapeutic levels of lithium appear to show an increase in IP synthase expression in the hippocampus but not in the frontal cortex (56) implying a regiospecific regulation in brain. Guan *et al.* (42) have observed that in HepG2 (liver-derived) cells, glucose and lovastatin increase mRNA expression, the latter invoking a G-protein-coupled signal transduction system. Our earlier work with the human promoter suggests that E2F1 can up-regulate gene expression (57). Clearly there are many interesting facets to IP synthase regulation that remain quite complex and poorly understood.

Adding to this complexity, genome databases such as the National Center for Biotechnology Information (NCBI) have identified novel IP synthase transcripts that have the potential to encode putative isoforms (58). More recently, some alternatively spliced transcripts of human IP synthase, associated with exon-skipping, have been found to be increased in the lymphocytes of bipolar patients who have had a family history of major psychiatric disorder (59). Herein, we report for the first time the identification and characterization of a number of isoforms in rat tissues, focusing primarily on a 16-kDa isoform, transcribed by an intron retention (IR) mechanism, that negatively regulates IP synthase function. Our findings resolve some of the molecular weight paradoxes observed with the native enzyme in various tissues and raise intriguing questions about the role of this enzyme in inositol homeostasis and its dysregulation in psychiatric disorders.

## EXPERIMENTAL PROCEDURES

**Materials**—Unless specified, reagents were of analytical grade procured from established manufacturers. Fetal rat tissues (21-day gestation) were obtained from Zivic Laboratories (Zelienople, PA). Normal adult brain tissues (cerebellum and amygdala from a 50-year-old female; hypothalamus and Brodmann Area 10 from 50- to 51-year-old males) were obtained from the Harvard Brain Tissue Resource Center, Boston, MA, after approval by the R & D Committee, Veterans Affairs Medical Center, Louisville, KY. Cell culture media, penicillin-streptomycin, and fetal bovine serum were from Invitrogen (Rockville, MD) or ATCC (Manassas, VA).

**Cell Culture**—Serum-free HeLa cells (ATCC No. CCL-2.3) were grown in RPMI 1640 media containing 2% TCH (Celox Laboratories, Inc., St. Paul, MN); SK-N-AS cells (ATCC No. CRL-2137), derived from a human neuroblastoma cell line, were grown in high glucose Dulbecco's modified Eagle's medium containing 10% fetal bovine serum; HEK (Human embryonic kidney) 293 cells (ATCC CRL-1573) were grown in FreeStyle 293 medium containing 4 mM GlutaMax (Invitrogen). All cell lines were grown in the presence of penicillin and streptomycin.

**Northern Blot Analysis**—A rat multiple tissue Northern blot from Clontech Laboratories, Inc. (Palo Alto, CA) was used. A full-length *Isyna1* cDNA fragment was random-labeled using the Prime-a-Gene labeling system (Promega, Madison, WI) and

[ $\alpha$ - $^{32}$ P]dCTP (Amersham Biosciences, Piscataway, NJ) and purified through a Microspin G-25 column (Amersham Biosciences). The blot was prehybridized in 0.5 M sodium phosphate buffer, pH 7.2/7% SDS for 2 h at 65 °C and then hybridized with the same buffer containing  $1 \times 10^6$  cpm/ml of the labeled probe overnight. The blot was washed for 10 min at room temperature in  $1 \times$  SSC/0.1% SDS and then at 68 °C. This was followed by two stringent washes at 68 °C in  $0.1 \times$  SSC/0.1% SDS for 10 min, after which the blot was enclosed in Saran wrap, placed in a Kodak X-Omatic cassette, and exposed at -70 °C for 1–4 days. The blot was stripped by incubating in 0.5% SDS for 10 min in a boiling water bath and reprobed with a  $^{32}$ P-labeled PCR-amplified rat  $\beta$ -actin cDNA fragment (60).

**Total RNA Isolation and cDNA Synthesis**—About 50–100 mg of tissue or  $1 \times 10^7$  cells was used for the isolation of total RNA by employing either the TRIzol method (Invitrogen) or the RNeasy Mini kit (Qiagen, Valencia, CA). Tissues were homogenized with a VirTishear (Virtis, Gardiner, NY) in Falcon 2059 tubes containing the appropriate buffer, while cells were scrapped off dishes, counted, and passed five times through a 19½-gauge needle. 1  $\mu$ g of total RNA was treated with RQ1 DNase (Promega) at 37 °C for 20 min, inactivated at 70 °C for 15 min, and then used for oligo(dT)-primed cDNA synthesis using the Thermoscript RT-PCR system (Invitrogen).

**PCR**—PCR was carried out in a PerkinElmer Life Sciences Cetus DNA Thermal cycler using TaqDNA polymerase (Promega, Madison, WI) according to the manufacturer's instructions. Two primer sets were used for amplifying rat cDNA sequences: R-ss2 (exon 4, 5'-CAACGACCTGGTGTGGTGGATG) with R-as2 (exon 6, 5'-ACGATGACCTTGTC-CAATCC), and R-ATGXhoI (exon 2, 5'-TCGCTCGAGGC-GATGGAGCCTGCCGCCGAGAT) with R-as3 (exons 6/7, 5'-CCAGGCCAAGCTGGATAGTA). The PCR profiles were 94 °C/2 min, followed by 35 cycles at 94 °C/30 s, 50 °C/45 s, and 72 °C/45 s for the former (amplicon size: 368 bp with intron 4 and 279 bp without) and at 52 °C annealing temperature for the latter (amplicon size: 871 bp with intron 4 and 782 bp without). For humans, H-P2 (exon 3/4, 5'-GGAGGCCAAGCTACTACGGCT) with H-14TAA EcoRI (intron 4, 5'-GGGAATTCCTCACTCGGCCCTGCCCGGATC) for the  $\gamma_c$  cDNA (224-bp amplicon), and H-402 (exon 4, 5'-GAGGTGTTCGTACCCTTCAG) with H-598 (exon 5, 5'-AATTCGGGGATGTAAACAGA) for the  $\alpha$  cDNA (192-bp amplicon) were used. PCR, as above, was at an annealing temperature of 50 °C. Because these primers were modified for other use, some carried nt mismatches (underlined) or restriction enzyme sites.

**Southern Blot Analysis**—PCR products were resolved on 1.2% agarose gels and transferred to Zeta-Probe GT membranes (Bio-Rad, Hercules, CA) according to the manufacturer's protocol. The DNA was cross-linked to the membrane at 5000  $\mu$ J/cm<sup>2</sup> in a GS Gene linker UV chamber (Bio-Rad). Probe preparation, membrane hybridization, and processing were as described for Northern blot analysis.

**Purification of Rat Testes IP Synthase**—All purification steps were carried out at 4 °C. About 145 g of decapsulated rat testes were homogenized in a Potter-Elvehjem glass Teflon homogenizer in two volumes of 50 mM Tris-HCl, pH 7.5 (standard) buffer and centrifuged at  $100,000 \times g$  in a Beckman-L8 Ultra-

centrifuge. The clear supernatant was subjected to ammonium sulfate (20–40%) fractionation, and the pellet was dissolved in, and dialyzed against, the standard buffer overnight at 4 °C. The supernatant obtained after centrifugation at  $10,000 \times g$  for 20 min in a Sorvall RC5B centrifuge was loaded onto a Q-Sepharose (Amersham Biosciences) column (50 ml, equilibrated with 20 mM Tris-HCl, pH 7.5) and eluted with a KCl gradient in the same buffer until a concentration of 0.5 M KCl was reached. 10-ml fractions were collected and assayed for IP synthase activity (33). The active fractions were pooled and loaded onto a G6P affinity column (1.5  $\times$  15 cm), prepared as previously described (33) in standard buffer, and eluted with a salt gradient of 0.3 M KCl. IP synthase activities were assayed for all fractions, and peak fractions were pooled. A portion of the pooled enzyme was passed through a Bio-Gel column (Bio-Rad, 2.5  $\times$  91 cm, total column volume, 447 ml), and 10-ml fractions were collected. Fractions with peak enzyme activity were analyzed by SDS-PAGE and stained with Coomassie Blue for purity assessment. Some of these fractions were used for antibody preparation (see below).

**Partial Purification of IP Synthase from Various Tissues for SDS-PAGE Analysis**—Decapsulated rat testes (155 g) from Sprague-Dawley rats were homogenized in 310 ml of ice-cold 0.154 M KCl containing 0.2 mM dithiothreitol and a protease inhibitor mixture (Roche Applied Science) using a blender. The homogenate was centrifuged at 13,000 rpm for 2 h at 4 °C using a GSA rotor in a Sorvall RC5B centrifuge. To the clear supernatant, ammonium sulfate was added to 30% saturation and stirred at 4 °C for 1 h. After centrifugation, as above, the clear supernatant was subjected to 40% ammonium sulfate saturation. The pellet obtained after centrifugation was dissolved in 50 mM Tris-HCl, pH 7.0 buffer and loaded onto a 16/10 HiTrap phenyl-Sepharose column (Amersham Biosciences) equilibrated with 25% ammonium sulfate in 50 mM Tris-HCl, pH 7.0, containing 0.2 mM dithiothreitol. After washing extensively with the equilibrating buffer, the bound proteins were eluted with a 25–0% linear gradient of ammonium sulfate in the same buffer. 5-ml fractions were collected, and IP synthase-containing fractions were identified by Western blot analysis using the R-10 antibody (see below). These fractions were pooled, dialyzed against 50 mM Tris acetate, pH 7.4, buffer and passed over a Q-Sepharose column equilibrated with Tris acetate buffer. After washing with the same buffer, bound proteins were eluted with a 0–0.3 M linear gradient of NaCl in Tris acetate buffer. Fractions of 4 ml were collected. The active fractions containing IP synthase activity were resolved into two peaks of activity. The first (Peak I) represented partially purified IP synthase containing both the 68-kDa  $\alpha$  and the 16-kDa  $\gamma_c$  isoforms, whereas the second (Peak II) represented only the 68-kDa  $\alpha$  isoform devoid of the  $\gamma_c$  isoform (see "Results"). Peak II fractions were pooled and concentrated by ammonium sulfate precipitation and dialyzed in Tris acetate buffer. These fractions were used for IP synthase activity determinations. Peak fractions were analyzed by Western blotting using the R-10 antibody and stored at -70 °C in the presence of 0.02% sodium azide. Pancreas (~5 g) and intestine (~210 g, cut into 1-inch pieces) pooled from several rats were processed similarly, except that the ammonium sulfate precipitate between 25 and 50% satura-



## myo-Inositol-3-phosphate Synthase Isoforms

tion was used. Purification was carried out until the phenyl-Sepharose column chromatography step, and IP synthase fractions (5 ml) were identified by Western blotting and stored as described above. Rat brains (~25 g) were purified similarly, and the ammonium sulfate precipitate was fractionated on a BioGel (100 × 15 cm) column. Fractions of 5 ml were collected, identified for IP synthase activity, and stored as before.

**Generation of the R-10 Polyclonal IP Synthase Antibody**—Electrophoretically homogeneous rat testis 68-kDa protein (see above) was used to raise polyclonal antibodies in New Zealand White rabbits. Rabbits were maintained for 5–7 weeks, and immunoglobulins from rabbit serum were purified using HiTrap Protein G HP 1-ml columns (Amersham Biosciences) following the manufacturer's instructions.

**Western Blot Analysis**—Protein concentrations were determined by the BCA protein assay (Pierce). Typically, 50 μg of the protein was resolved by 10–12.5% (w/v) SDS-PAGE and transferred to polyvinylidene difluoride (Bio-Rad) membranes. Blots were blocked with 5% dry milk in 0.5% Tween 20, 150 mM NaCl, and 50 mM Tris-HCl, pH 7.4 (TTBS buffer), for 1 h at room temperature and then incubated with a 1:1000 dilution of the R-10 antibody in TTBS buffer for 1 h at room temperature. A 1:2000 dilution of secondary goat anti-rabbit IgG conjugated with alkaline phosphatase (BioSource International, Inc., Camarillo, CA) was applied to the blot for 1 h at room temperature, and the signals were visualized with the 5-bromo-4-chloro-3'-indolyl phosphate/nitro blue tetrazolium chromogenic reagent.

**Mass Spectrometry Analysis**—Rat testis IP synthase fractions identified after the phenyl-Sepharose purification step (see above) were concentrated by lyophilization. The sample was dissolved in gel loading buffer and resolved preparatively by SDS-PAGE in a Sturdiel Vertical slab gel unit (13 × 16 cm, Hoeffer, Inc., San Francisco, CA). After electrophoresis, proteins were visualized with Coomassie Brilliant Blue R-250, and bands in the vicinity of the 20-kDa molecular mass marker were excised from the gel, minced into ~1-mm pieces, and submitted to the University of Louisville mass spectrometry core facility for analysis. Briefly, the gel pieces were treated with iodoacetamide to alkylate cysteine residues and then subjected to "in-gel" trypsin digestion according to established methods (61). Mass spectra were collected on a TOF Spec 2E instrument from Micromass (Waters) Corp. (Milford, MA). The instrument was set to reflectron mode, the detector in positive ion mode, and data recorded from 0 to 4000 Da. Ions less than 500 Da were subjected to ion suppression to enhance signal of larger peptide masses by suppressing peaks in the matrix region. Twelve spectra were collected automatically using set locations on each sample well. Each spectrum consisted of 40 laser firings, and all 12 spectra, a total of 480 laser firings, were averaged into one to achieve better signal-to-noise ratios. All spectra were processed with Mascot Distiller from Matrix Sciences, Ltd. prior to database searching. The spectra were checked and adjusted for mass accuracy using internal matrix and trypsin autolysis peaks. For MS searches the Peptide Mass Fingerprint program was used with a peptide mass tolerance of 75 ppm. The 62 and 68-kDa polypeptides from the intestine and testis, respectively, processed similarly by SDS-PAGE and Coomassie

Brilliant Blue staining, were commercially analyzed by Dr. John Leszyk, Proteomics and Mass Spectrometry Lab, University of Massachusetts, Worcester, MA.

**Bacterial Expression and Purification of Rat  $\gamma_c$  Isoform**—A PCR-amplified intact coding region of rat  $\gamma_c$  cDNA was ligated to pRSET-A vector (Invitrogen), and the resulting plasmid was transformed into Novagen's Rosetta (DE3) pLysS (EMD Chemicals, Inc., Gibbstown, NJ) cells. A single colony was picked and inoculated into 5 ml of LB containing 50 μg/ml carbenicillin and 32 μg/ml chloramphenicol. The culture was incubated at 37 °C overnight and then inoculated into 1 liter of fresh LB media containing both antibiotics. When the culture had attained an optical density of 0.5 at  $A_{600}$ , it was induced with 0.5 mM isopropyl 1-thio- $\beta$ -D-galactopyranoside and allowed to grow for a further 3 h. Cells were pelleted and suspended in 50 mM Tris-HCl, pH 7.8, containing 5 mM EDTA and 1 mM phenylmethylsulfonyl fluoride and lysed by passing three times through a French Press Cell Disrupter (Glen Mills Inc., Clifton, NJ, 1000 p.s.i.). The inclusion bodies containing the  $\gamma_c$  isoform were collected by centrifugation and washed twice with Tris-HCl buffer containing 2% sodium deoxycholate. After removal of residual detergent with a water wash, the inclusion bodies were dissolved in 25 ml of 50 mM sodium phosphate buffer, pH 8.0, containing 6 M urea, 300 mM NaCl, and 1 mM dithiothreitol (binding buffer). The sample was mixed at room temperature for 2 h and then centrifuged at 13,000 rpm in a Sorvall RC5B centrifuge. The clear supernatant was loaded onto a 5-ml HisTrap FF column (Amersham Biosciences) equilibrated with the binding buffer. After extensive washing with the binding buffer, the bound  $\gamma_c$  isoform was eluted with a linear gradient of 0–500 mM imidazole in the binding buffer. 3-ml fractions were collected, and fractions containing the  $\gamma_c$  isoform were identified by SDS-PAGE. Enzyme fractions were pooled and dialyzed extensively, first against 50 mM Tris-HCl, pH 9.0, containing 5 mM  $\beta$ -mercaptoethanol and then against 50 mM Tris-HCl, pH 8.0, to refold the protein. Samples were aliquoted and stored at 4 °C for further analysis. To assess if proper folding had occurred, the binding of  $\text{NAD}^+$  to the enzyme was determined by measuring the absorption spectra from 220 to 340 nm in a NanoDrop ND1000 spectrophotometer, as previously described (62).

**IP Synthase Activity Assays Using Purified  $\alpha$  and  $\gamma_c$  Isoforms**—Bacterially purified, recombinant rat  $\gamma_c$  isoform was added to partially purified  $\alpha$  isoform to determine the effect on enzyme activity. The  $\alpha$  isoform derived from Peak II fractions after Q-Sepharose chromatography (as detailed above) was devoid of the  $\gamma_c$  isoform (see "Results"). Enzyme activity was determined as previously described (33). Briefly, a 500-μl reaction containing 50 mM Tris-HCl, pH 7.5, 4 mM G6P, 1 mM  $\text{NAD}^+$ , 10 mM ammonium chloride, and 200 μl of enzyme extract (4–8 mg of protein) was incubated at 37 °C for 1 h, after which 20% trichloroacetic acid was added to precipitate proteins. The resulting clear supernatant was treated with sodium periodate and sodium sulfite, and an aliquot was treated with malachite reagent. The color developed was read at  $A_{660}$ .  $A_{660}$  absorbance values were directly used as a measure of enzyme activity as all conditions and volumes used were similar. As an enzyme control, both bovine serum albumin and IgG were used, and nei-

ther was found to display biosynthetic activity with G6P. Both isoforms were used in equal (protein) amounts. The tested conditions were direct incubation of the isoforms with  $\text{NAD}^+$  without preincubation, preincubation of the two isoforms at  $37^\circ\text{C}$ , prior to the addition of  $\text{NAD}^+$ , and preincubation of the  $\gamma_c$  isoform with  $\text{NAD}^+$  for various times, prior to addition to the reaction containing the  $\alpha$  isoform. Experiments were done in triplicates using one-way analysis of variance with Bonferroni's multiple comparison test to determine statistical significance.

## RESULTS

**IP Synthase mRNA Expression in Rat Tissues**—A Northern blot analysis of rat tissue poly(A)<sup>+</sup> mRNAs confirms the very high expression of the *Isyna1* gene in testis (Fig. 1). Brain, lung, liver, and kidney exhibit moderately high expression, heart and spleen, low expression, and skeletal muscle, almost no expression. This expression pattern does not mirror completely that observed in human tissues (42) (see "Discussion"). A careful scrutiny of the blot indicates that the *Isyna1* probe hybridizes to two bands (Fig. 1, arrows) with the lower band corresponding to the fully spliced transcript encoding the 68-kDa subunit, because this is the most intense band in testis, inferred from a short exposure of the blot (see also Fig. 6B). The upper band, thus, represents a putative novel *Isyna1* mRNA. The available

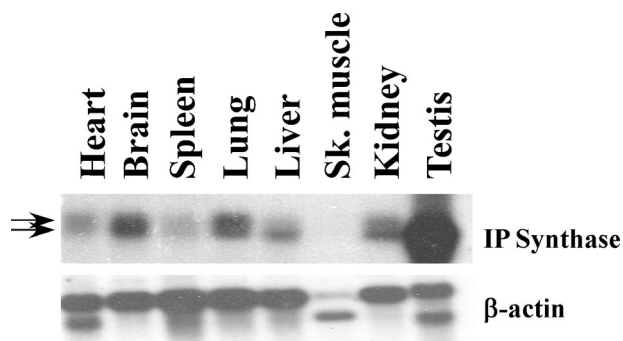


**FIGURE 1. Northern blot analysis of rat *Isyna1* gene expression.** A Northern blot containing poly(A)<sup>+</sup> mRNA from various rat tissues (Clontech Laboratories, Inc.) was probed with <sup>32</sup>P-labeled rat *Isyna1* full-length cDNA fragment.  $\beta$ -Actin was used as a control. Two closely migrating mRNAs can be distinctly identified (arrows). The lower band is the fully spliced mRNA encoding the 68-kDa polypeptide, whereas the upper band is a novel transcript. *Sk.*, skeletal.

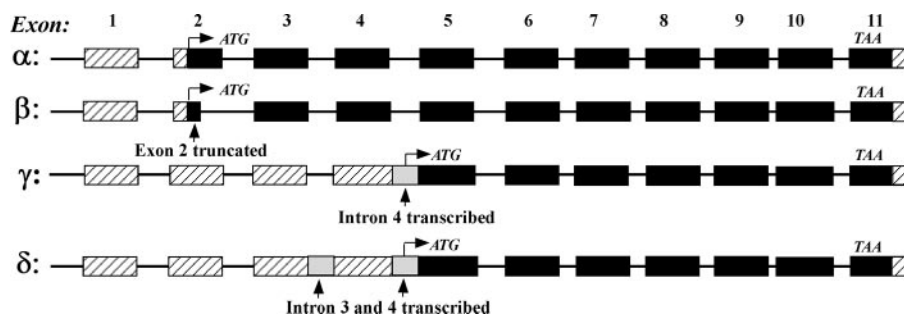


**FIGURE 2. Coding regions of IP synthase isoforms.** Coding and untranslated regions are shown as dark and hatched boxes, respectively. Translational start (ATG) and stop (TAA) codons are indicated. Transcribed introns are in gray boxes. Transcription of intron 4 in the  $\gamma$  transcript and introns 3 and 4 in the  $\delta$  transcript result in a novel ATG codon in intron 4 for both isoforms that is in-frame with downstream exons 5–11. The resulting ORF could potentially encode a 48-kDa polypeptide. The  $\beta$  transcript harbors an in-frame 54-nt deletion at the 3'-end of exon 2. The fully spliced  $\alpha$  mRNA encoding the 68-kDa polypeptide has been well studied (38, 42).

sequences in the NCBI database do not indicate the existence of another *Isyna1* genetic locus. This novel transcript, although variably expressed in different tissues, is generally less expressed than that encoding the 68-kDa polypeptide (Fig. 1). The identification of the novel transcript prompted us to undertake PCR analysis of cDNA samples derived from various tissues and a search of public databases, such as the NCBI, to confirm its identity and presence.

**Identification of Differentially Spliced Rat *Isyna1* Transcripts**—A search of the NCBI database and PCR amplification of cDNA products, utilizing primers targeted to different exons, yielded a number of variously spliced transcripts (Fig. 2), as determined by sequencing of some of the cloned products. We now term the ubiquitously expressed fully spliced mRNA, which encodes the 68-kDa polypeptide, as the " $\alpha$ " mRNA. Three additional transcripts called " $\beta$ ,  $\gamma$ , and  $\delta$ " were also identified (note: the  $\delta$  transcript was identified only by database search). The structure of the  $\alpha$  mRNA, derived from cDNAs and expressed sequence tags with gene accession numbers BC079011, CO561111, and NM\_001013880 indicate that the gene has 11 exons and 10 introns with the initiation and termination codons located in the second and eleventh exons, respectively (Fig. 2). The mRNA for the  $\beta$  form harbors an in-frame 54-bp deletion in exon 2 that occurs by a GC-AG splicing mechanism. It removes the last 18 amino acids (Ala<sup>23</sup>–Arg<sup>40</sup>; see also Fig. 5) encoded by this exon and can potentially encode for a 59-kDa polypeptide. This transcript identified in the testis and kidney by sequencing has not been reported elsewhere. The  $\gamma$  and  $\delta$  transcripts are extremely interesting, because they both arise from intron transcription generating mRNAs that are slightly larger than the fully spliced  $\alpha$  form. One or both of these could account for the larger mRNA species seen in the Northern blot (Fig. 1). The  $\gamma$  form arises by transcription of intron 4 (89 bases) and the  $\delta$  by transcription of both introns 3 and 4 (162 + 89 bases). Partial sequences for both these transcripts can be found in the NCBI database (gene accession numbers:  $\gamma$ : NM\_001013880, BC079011, CO561111, CO393821, CK653046, CK469762, and CO395123;  $\delta$ : CO563262 and CV108637). Both the  $\gamma$  and  $\delta$  transcripts can potentially encode an identical 48-kDa polypeptide, because of a large ORF (open reading frame) created by an in-frame ATG present in intron 4

(Fig. 2). Although we were able to identify and confirm the existence of the  $\beta$  and  $\gamma$  transcripts, the latter readily amplifiable from mRNAs derived from most tissues, the transcript for the  $\delta$  form was not detected in our PCR analysis. We conclude that the larger transcript seen in the Northern blot likely represents the predominantly expressed  $\gamma$  transcript, whereas those encoding the  $\beta$  and  $\delta$  isoforms presumably represent poorly expressed or rare transcripts. Hence, our focus was on the putative  $\gamma$  isoform.

## myo-Inositol-3-phosphate Synthase Isoforms

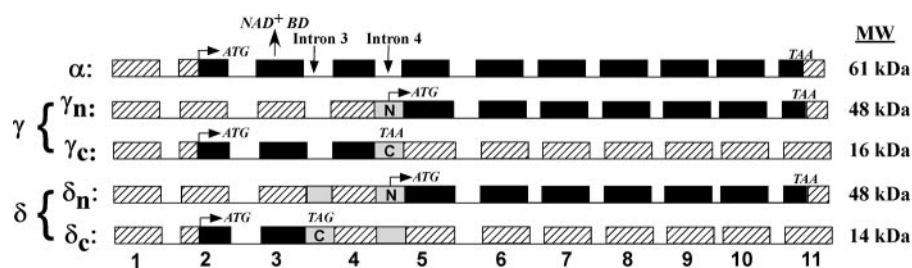


**FIGURE 3. The coding potential of the  $\gamma$  and  $\delta$  mRNAs.** The  $\gamma$  and  $\delta$  mRNAs can potentially encode for two isoforms each. For the  $\gamma$  isoform, transcription of intron 4 (gray box) can generate isoforms with either a novel N ( $\gamma_n$ ) or a novel C ( $\gamma_c$ ) terminus. The  $\gamma_c$  mRNA has a short ORF compared with  $\gamma_n$ . Similarly, transcription of introns 3 and 4 (gray boxes) in the  $\delta$  isoform can generate  $\delta_n$  or  $\delta_c$  mRNAs with novel N and C termini, respectively. Note that the  $\delta_n$  and  $\gamma_n$  mRNAs encode identical polypeptides. Coding exons (black boxes), non-coding exons (hatched boxes), start (ATG) and stop (TAA and TAG) codons are indicated. Exon numbers are indicated from the bottom. Downward arrows indicate the transcribed introns. The calculated molecular mass for each isoform is indicated on the right. The  $\text{NAD}^+$  binding domain (BD) is indicated by the third exon necessary for IP synthase activity is present only in the  $\alpha$ ,  $\gamma_c$ , and  $\delta_c$  isoforms.

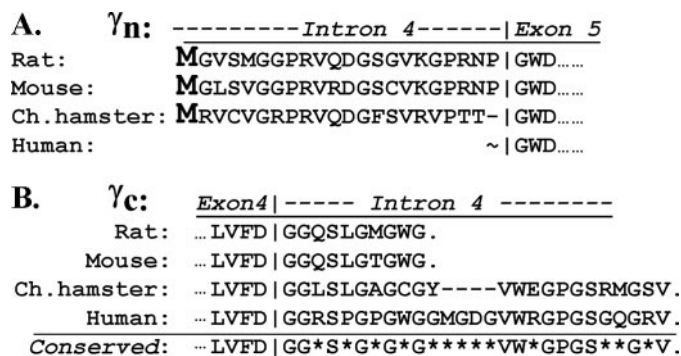


**FIGURE 4. The intron 4-encoded peptide is conserved in  $\gamma_c$  but not in  $\gamma_n$ .** The translated peptides derived from intron 4 transcription for  $\gamma_n$  and  $\gamma_c$  isoforms are shown. A, translation for  $\gamma_n$  isoform is initiated in intron 4 at the first methionine (bold M) shown, generating a 22-amino acid novel N-terminal peptide for rat and mouse that is in-frame with the IP synthase polypeptide encoded by exons 5–11. These peptides are not conserved in Chinese hamster and human (–, loss of a nt in the corresponding codon in Chinese hamster; ~, lack of an upstream ATG codon; see “Results”). B, for the  $\gamma_c$  isoform, translation begins at the “normal” AUG codon in exon 2 (not shown) and terminates with the intron 4 transcribed sequences, as shown, generating various C termini. Note the high conservation between all species, especially between Chinese hamster and human. The unique C terminus in all species is rich in glycine, the most conserved residue. Dashes in the Chinese hamster sequence are introduced for alignment.

**Properties of the Putative  $\gamma$  mRNA**—Transcription of intron 4 in the  $\gamma$  mRNA generates two ORFs that have sequence identity with IP synthase (Fig. 3): (i) a longer ORF, which begins with a novel ATG codon in intron 4, in-frame with downstream exons 5–11, and terminating at the “normal” stop codon in exon 11; this generates a putative 48-kDa isoform with a novel 22-amino acid N-terminal peptide (hereafter called the  $\gamma_n$  isoform), or (ii) a shorter ORF that begins with the normal ATG codon in exon 2 and terminating in an intron 4 stop codon, thus generating a putative 16-kDa isoform with an unique 10-amino acid C-terminus (the  $\gamma_c$  isoform). The mRNAs encoding the  $\gamma_n$  and  $\gamma_c$  isoforms are exactly identical in structure except that the former has seven coding exons and the latter three. The only difference between the  $\gamma_n/\gamma_c$  mRNAs and the  $\alpha$  mRNA is the presence of an intact intron 4, as evidenced by our ability to amplify intact intron 4 containing cDNAs from exons 2–11 from testis, brain, and kidney (data not shown). Thus,  $\alpha$  mRNA exons that are no longer peptide-coding have become 5'- or 3'-untranslated regions in  $\gamma_n$  or  $\gamma_c$  mRNAs, respectively. A sim-

ilar case can be made for the  $\delta$  isoforms, which by virtue of retaining introns 3 and 4 in their mRNAs produce  $\delta_n$  or  $\delta_c$  transcripts (Fig. 3; see “Discussion”). Note that  $\gamma_n$  and  $\delta_n$  encode the same 48-kDa isoform. For the  $\gamma$  isoforms, the presence of a larger ORF would suggest that it is the  $\gamma_n$ , rather than the  $\gamma_c$ , isoform that is expressed. To ascertain this, we compared intron 4 derived N-terminal peptide sequences of the  $\gamma_n$  isoform from mouse, rat, Chinese hamster (Chinese hamster ovary cell line), and human (sequences were from the NCBI

database or from sequencing PCR-amplified cDNAs). Surprisingly, this peptide was not evolutionarily conserved (Fig. 4A). Although the rat and mouse sequences were highly conserved, the peptide sequence was not in-frame in Chinese hamster due to a frameshift in the last codon of intron 4, and in human, an ATG codon in-frame with downstream exons 5–11 could not be found (even if one goes into upstream exons). This questions the existence and viability of the  $\gamma_n$  isoform. We next examined the intron 4-encoded C-terminal peptides of the putative  $\gamma_c$  isoform from all 4 species (Fig. 4B). Although the peptides differ in amino acid length (rat and mouse: 10; Chinese hamster: 23; and human: 27), all of them display a very high level of sequence conservation. More compelling is the observation that 14/27 residues in Chinese hamster are fully conserved in human. The C-terminal peptides are extremely glycine-rich (50% in mouse and rat, 35% in Chinese hamster, and 44% in human) with glycine being the most conserved residue (57%). These observations provide strong support for the expression of  $\gamma_c$ , rather than  $\gamma_n$ , as the intron 4-encoded polypeptide. The nt and amino acid sequences of the  $\alpha$ ,  $\beta$ ,  $\gamma_c$ , and  $\gamma_n$  isoforms are depicted in Fig. 5.

**Expression of the  $\alpha$  and  $\gamma_c$  Isoforms in Various Tissues**—Because the  $\alpha$  and  $\gamma_c$  mRNAs appear to be predominantly expressed (Fig. 1), we examined their mRNA expression by PCR analysis of cDNAs in various rat tissues (including various brain regions). Intron 4 flanking primers capable of amplifying both the  $\alpha$  and  $\gamma_c$  mRNAs were used. Because, some of the  $\gamma_c$  bands were faint on routine agarose gel analysis, these gels were Southern-blotted and detected using radioactively labeled *Isyna1* cDNA (Fig. 6A). Both the  $\alpha$  and  $\gamma_c$  mRNAs are detectable in most tissues to various extent. In intestine, lung, liver, and muscle, the  $\gamma_c$  mRNA appears to be predominantly expressed. In testis, spleen, and cortex the  $\alpha$  mRNA predominates, whereas both transcripts appear to be equally expressed in brain stem, hippocampus, cerebellum, and amygdala (Fig. 6, A and B). Although not quantitative, these results indicate that the two isoforms are differentially expressed in various rat tissues. These intriguing observations prompted us to examine if these isoforms display temporal expression during development. Examination of brain, heart, kidney, lung, and liver tissues from fetal rats (at 21-day gestation) reveals that both isoform mRNAs are similarly expressed during early development



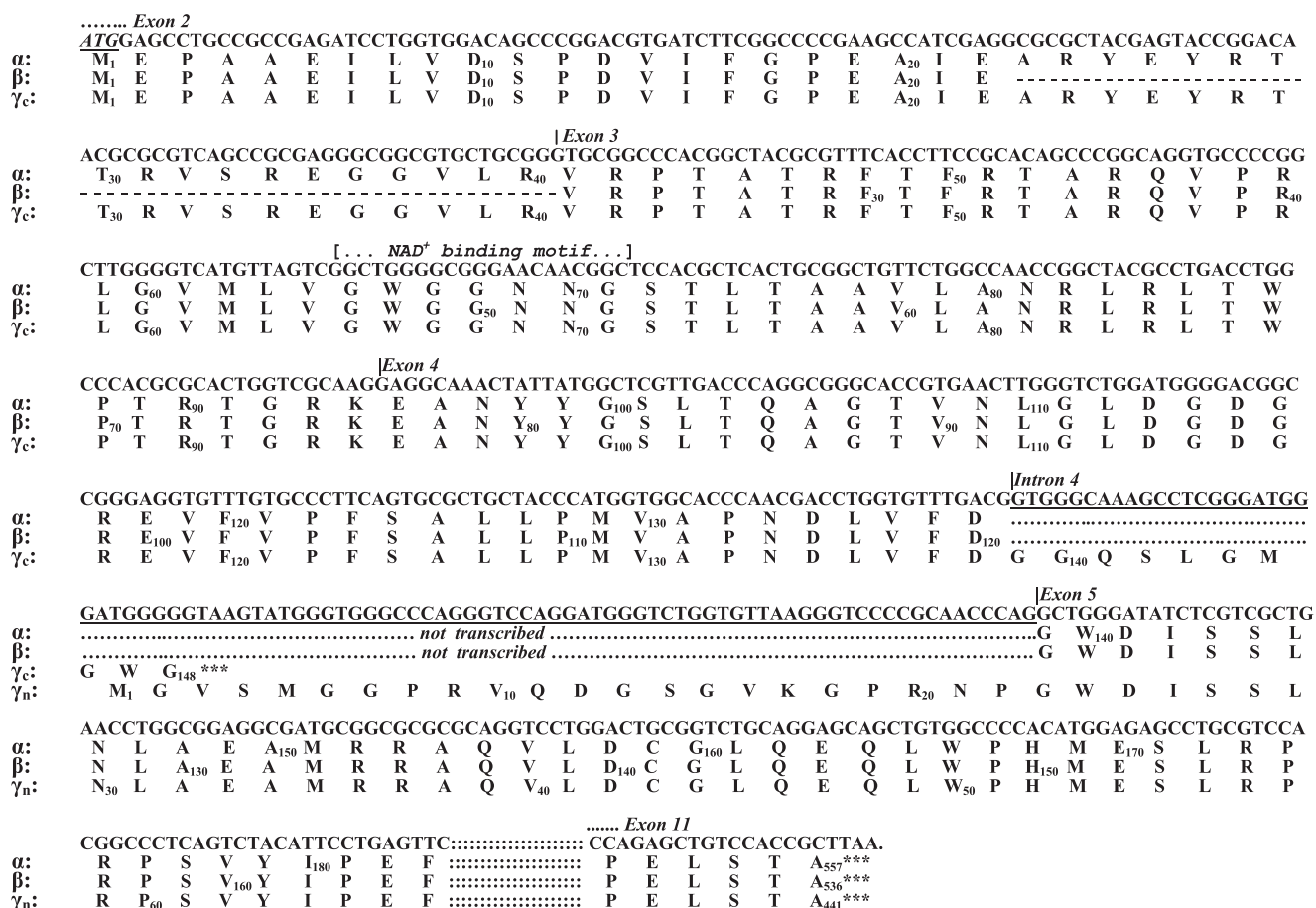


FIGURE 5. Nucleotide and amino acid sequences of the  $\alpha$ ,  $\beta$ ,  $\gamma_c$ , and  $\gamma_n$  isoforms. Only regions showing differences in the four isoforms are depicted. The nt sequence depicted extends from exon 2 to part of exon 5, including intron 4; part of exon 11 is shown to depict the stop codon in longer isoforms. The remaining exonic regions, depicted by *colons* at the bottom, are derived from 762 bp of cDNA encoding 254 amino acids and are not shown as these are identical to the  $\alpha$  isoform, available in the NCBI database (gene: *Isyn1*; gene ID: 290651). Every 10th amino acid is numbered beginning with the first methionine (M<sub>1</sub>), and each amino acid is centered below the corresponding codon. The intronic sequence is *underlined*. The *dotted lines* below the intronic sequence indicate regions that have been spliced out, and therefore not transcribed, in the  $\alpha$  and  $\beta$  transcripts; the *dashed lines* in the  $\beta$  isoform indicate deleted amino acids; *asterisks* indicate stop codons. the amino acid sequence in parenthesis in the 3rd exon, -GWGNG-, is the putative NAD<sup>+</sup> binding motif.

with  $\alpha$  being more predominant than  $\gamma_c$  (Fig. 7A, arrows). The *topmost band* seen in this figure is hybrid DNA comprising both amplicons (confirmed by sequence analysis) and is typically observed when co-amplifying two sequences of identical homology. To ensure that the  $\gamma_c$  isoform is expressed in humans, we examined several human cell lines, such as HeLa (epithelial), SK-N-AS (neuroblastoma), and HEK (human embryonic kidney), and various human brain regions, such as amygdala, cerebellum, hypothalamus, and Brodmann Area 10 of the cortex. In the case of humans, the intron 4-flanking primers amplified only the shorter  $\alpha$  mRNA (192 bp) but not the larger  $\gamma_c$  transcript (data not shown). However, when an intron 4-specific primer was used, an amplicon (224 bp) signifying the presence of the  $\gamma_c$  transcript was seen in all cases (Fig. 7, B and C). The inability of the human primers to amplify both isoforms simultaneously, unlike in rat, may indicate either a preferential amplification of the shorter  $\alpha$  mRNA or to low levels of  $\gamma_c$  mRNA in human tissues. In these experiments, total RNAs were always treated with DNase I (RNase-free) prior to cDNA synthesis to rule out amplification of any contaminating genomic DNA (see "Experimental Procedures"). Additionally, PCR analysis of cDNAs did not identify other intronic

sequences even though the sizes of many are small (~100 bp; see below).

*Identification of the  $\gamma_c$  Polypeptide in Rat Tissues*—While our observations thus far provide convincing evidence for the existence of the intron 4-containing  $\gamma_c$  mRNA, we wanted to examine whether this is translated into the cognate 16-kDa polypeptide. IP synthase has been purified innumerable times in our laboratory from rat tissues in the past. We, therefore, sought past enzyme purification data for evidence of a putative 16-kDa polypeptide in purified IP synthase preparations. Fig. 8A depicts a Coomassie Blue-stained SDS-PAGE gel of rat testes IP synthase resolved after purification by G6P affinity chromatography (see "Experimental Procedures"). The eight lanes (*Fractions 15–22*) depict fractions exhibiting maximal IP synthase activities. An intense band consistent with the  $\gamma_c$  isoform (at ~20 kDa) is found copurifying with the major 68-kDa  $\alpha$  isoform with enrichment of both polypeptides in *Fraction 18*. Note that the theoretical and apparent molecular mass differ for these isoforms (see below for molecular mass assignments for the isoforms). A 32-kDa band is also seen spanning all lanes but it is present maximally in *Fraction 17*, not *Fraction 18*. To further resolve these bands, *Fractions 16–20* were pooled and sub-

## myo-Inositol-3-phosphate Synthase Isoforms

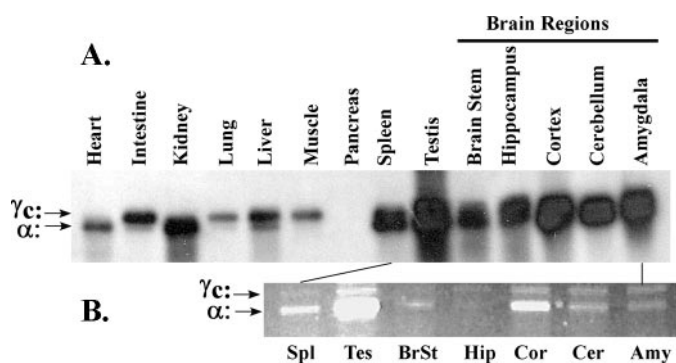


**FIGURE 6. Expression of  $\alpha$  and  $\gamma_c$  mRNAs in various rat tissues and rat brain regions.** *A*, cDNAs from various tissues were PCR amplified with intron 4-flanking primers, resolved on agarose gels, Southern blotted onto a Zeta-Probe (Bio-Rad) membrane, and probed with a  $^{32}\text{P}$ -labeled full-length rat *Isyn1* cDNA. Although not quantitative, the very high expression in testis is clearly evident. Both isoforms appear to be expressed in all brain regions and in most tissues to variable extent (see *panel B* for better resolution of bands). Notably, the  $\alpha$  mRNAs appear to be poorly expressed or absent in intestine, lung, and muscle, whereas the  $\gamma_c$  mRNA is poorly expressed or absent in heart and kidney. Pancreatic mRNAs are apparently degraded, because  $\beta$ -actin (control) is also not amplifiable in this tissue (data not shown). *B*, because of overexposure in the last seven lanes (spleen to amygdala) due, in part, to the close migration of the two amplicons, the ethidium bromide-stained agarose gel prior to blotting is shown. The PCR bands representing both isoforms can clearly be seen in all lanes, including the brain stem and hippocampus. Note the high expression of the  $\alpha$  mRNA in testis.

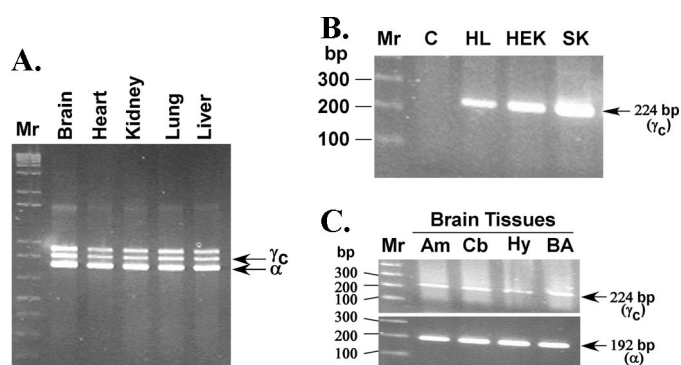


**FIGURE 7. Expression of  $\alpha$  and  $\gamma_c$  mRNAs in various rat and human tissues.** *A*, expression in fetal rat tissues (at 21 days gestation). PCR-amplified cDNAs with intron 4-flanking primers were resolved on agarose gels. The  $\alpha$  and  $\gamma_c$  amplicons are indicated. The unlabeled top band is a hybrid resulting from crossing over during amplification of  $\alpha$  and  $\gamma_c$  cDNAs and is typically observed in amplifying DNAs with high sequence homology. *B*, expression in human cell lines. PCR amplification of cDNAs with  $\gamma_c$ -specific primers yields an expected product of 224 bp. Cell lines: HL, HeLa; HEK, human embryonic kidney; SK, SK-N-AS neuroblastoma; C, water control; and Mr, 100-bp DNA marker. *C*, expression in human brain regions. PCR amplification of cDNAs with isoform-specific primers is shown.  $\gamma_c$  (224 bp) and  $\alpha$  (192 bp) amplicons are depicted in the top and bottom panels, respectively. Am, amygdala; Cb, cerebellum; Hy, hypothalamus; BA, Brodmann Area 10; and Mr, 100-bp DNA marker.

jected to Biogel P-100 gel filtration (Fig. 8B). The 68- and 20-kDa polypeptides still remain inseparable, in apparent stoichiometry, as evidenced by their comigration and manifesting peaks in the same fraction (*Fraction 24*), whereas the bulk of the 32-kDa polypeptide has moved to *Fractions 30–32* and does not remain with the active IP synthase fraction (all fractions were assayed for IP synthase activity). The 32-kDa polypeptide could be a proteolytic product or another isoform of IP synthase that is loosely bound to the enzyme complex. These data pro-

vide strong evidence, but do not necessarily prove, that the 20-kDa band is the  $\gamma_c$  polypeptide.

We next asked if a rabbit polyclonal antibody (R-10) raised against the 68-kDa  $\alpha$  isoform could detect this 20-kDa polypeptide. For this purpose, we used rat intestine not only because this tissue is highly enriched for the  $\gamma_c$  mRNA, but also because it appeared to lack the  $\alpha$  isoform (Fig. 6A). Partially purified IP synthase preparations from intestine were resolved on SDS-PAGE gels and probed with the R-10 antibody (Fig. 9A). Three IP synthase polypeptides were identifiable, one of which is consistent with the  $\gamma_c$  polypeptide at 20 kDa. The results also confirm the complete absence of the 68-kDa  $\alpha$  isoform in the intestine and the appearance of two new polypeptides of 62 and 43 kDa (see also Fig. 9B). The IP synthase polypeptide data (Fig. 9A) are consistent with the mRNA expression results (Fig. 6A) and suggest that IP synthase probably exists as a complex of distinct isoforms in the intestine. These observations and the efficacy of the R-10 antibody to detect various IP synthase polypeptides prompted us to examine the overall IP synthase isoform pattern in additional tissues. Fig. 9B shows partially purified enzyme extracts from pancreas, brain, intestine, and testis resolved on SDS-PAGE gels. The samples were intentionally overrun, because preliminary data indicated that much of the isoform differences occurred  $>35$  kDa. For testis (*lane 4*), two IP synthase bands are discernible, one of which is the expected  $\alpha$  isoform (68 kDa) and the other a closely migrating 66-kDa polypeptide. Indeed, this doublet pattern has been previously observed by Maeda and Eisenberg in their characterization of the rat testes enzyme (38). The figure clearly indicates that each tissue manifests a unique IP synthase isoform expression profile: pancreas, 67 kDa; brain, 68 kDa ( $\alpha$ ); intestine, 62 and 43 kDa; and testis, 68 kDa ( $\alpha$ ) and 66 kDa; this is in addition to the  $\gamma_c$  isoform present in brain, intestine, and testis (see Figs. 6 and 9A), which were run out of this gel.

**Identification of the  $\gamma_c$  Isoform Polypeptide by MS Analysis**—A partially purified enzyme extract from rat testes was used for the quantitative isolation of the putative 20-kDa polypeptide from a Coomassie Blue-stained SDS-PAGE gel and subjected to MALDI-TOF MS analysis. Our primary aim was to identify if any of the peptide(s) detected in this fragment were consistent with the presence of the  $\gamma_c$  isoform. Two adjacent bands submitted for analysis revealed the presence of four IP synthase peptides. These tryptic peptides (Peptides I to IV) are shown in Table 1, along with their calculated mass-to-charge ratio ( $m/z$ ) and their observed values in the ionic state  $[\text{MH}]^+$ . The analysis indicates that all four peptides are derived only from exons 2–4 (Peptide I from exons 2/3, Peptides II and III from exon 3, and Peptide IV from exons 3/4). Identification of peptide sequences from exons other than 2–4 would have argued against the presence of the  $\gamma_c$  isoform. Given the exon coverage and the size of this polypeptide, the data leave little room for the expression of any other IP synthase isoform except the  $\gamma_c$  isoform.

**Characterization of the Bacterially Expressed Recombinant Rat  $\gamma_c$  Isoform**—To examine the effect of the  $\gamma_c$  isoform on IP synthase activity, we cloned the coding region of the  $\gamma_c$  isoform into a plasmid, expressed it in bacteria, and purified the protein. A nearly homogenous preparation of rat  $\gamma_c$  isoform was



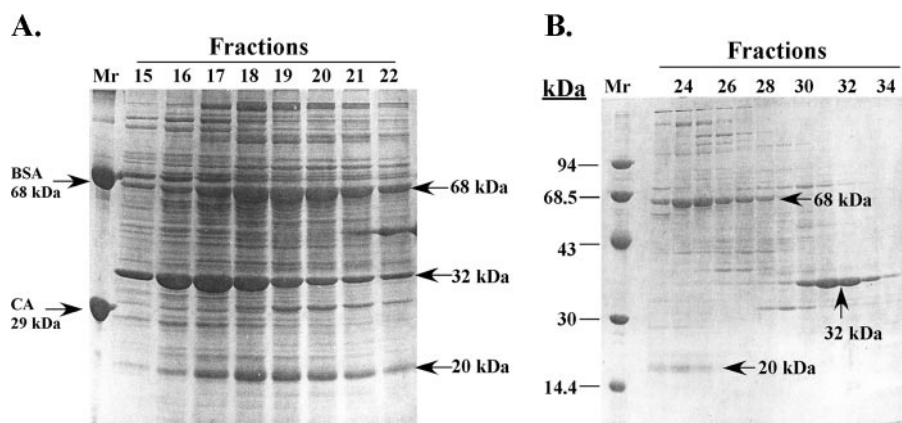


**FIGURE 8. Identification of the putative  $\gamma_c$  isoform in purified rat testes IP synthase.** *A*, fractions collected after G6P affinity chromatography were resolved on 12% SDS-PAGE (see “Experimental Procedures”). The 68- and 20-kDa bands (arrows, right) comigrate with maximal amounts of both polypeptides found in the 18th fraction. The presence of the 20-kDa protein is consistent with the  $\gamma_c$  isoform. A co-purifying 32-kDa protein (arrow, right) shows maximum intensity in the 17th fraction and does not comigrate with the  $\alpha$  form. The gel was stained with Coomassie Blue. BSA, bovine serum albumin; CA, carbonic anhydrase. *B*, Fractions 16–20 from *A* were pooled and further purified by gel filtration chromatography on Biogel P-100 and resolved on 12% SDS-PAGE. The 20-kDa polypeptide (the putative  $\gamma_c$  isoform) continues to comigrate with the 68-kDa  $\alpha$  isoform with peak band intensities, for both, in the 24th fraction. The 32-kDa protein, however, does not elute with the  $\alpha$  isoform and shows a peak in the 31st fraction. Enzyme activity of each fraction was determined as described (33). Bands were stained as in *A*. Molecular mass markers are indicated on the left.

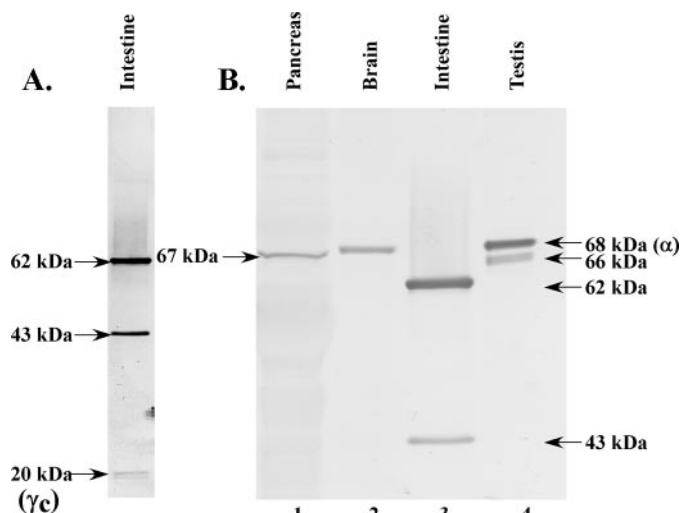


**FIGURE 9. Detection of  $\gamma_c$  and other novel protein isoforms in various rat tissues by Western blot analysis using an IP synthase-specific antibody.** IP synthase from various tissues was partially purified as described under “Experimental Procedures” and resolved on 12% (*A*) or 10% (*B*) SDS-PAGE. The molecular mass of each isoform is indicated. *A*, the 20-kDa polypeptide (the putative  $\gamma_c$  isoform) is detected by the R-10 IP synthase-specific antibody in the intestine, clearly indicating that it is an IP synthase isoform. Note the complete absence of the 68-kDa  $\alpha$  isoform in intestine (see also lane 3 in *B*). *B*, IP synthase preparations from various tissues were intentionally overrun to discriminate the high molecular mass isoforms present in pancreas (lane 1), brain (lane 2), intestine (lane 3), and testis (lane 4). Only the brain and testis manifest the 68-kDa  $\alpha$  isoform, whereas the pancreas has a slightly smaller isoform at 67 kDa. The intestine has a completely unique isoform profile comprising 62- and 43-kDa isoforms (as seen in *A*).

obtained after solubilizing inclusion bodies with 6 M urea and purifying through a nickel (HisTrap) column (Fig. 10, lane 9; Fig. 12, lane 2). The imidazole-eluted enzyme was refolded by gradual decrease in urea and pH levels. The recombinant protein migrated as a slightly larger polypeptide (23 kDa) because of the presence of an N-terminal fusion peptide harboring the 6 × His tag (Fig. 10). Typically, ~5 mg of  $\gamma_c$  polypeptide was

obtained from 1 liter of culture. Because the  $\gamma_c$  isoform lacks the catalytic domain, it was not expected to exhibit IP synthase activity (subsequently confirmed; see below). Therefore, to assess if the recombinant protein had folded correctly, and therefore biologically relevant, we determined if it would bind  $\text{NAD}^+$ , and cause a characteristic “blue shift” in the UV absorption spectra of the protein. Fig. 11 depicts UV absorption spectra of refolded  $\gamma_c$  polypeptide in the presence and absence of 20  $\mu\text{M}$   $\text{NAD}^+$ . Incubation with  $\text{NAD}^+$  causes a shift of the unbound  $\gamma_c$  isoform peak from 278 to 265 nm indicating that a conformational change had occurred upon  $\text{NAD}^+$  binding; denatured  $\gamma_c$  polypeptide did not exhibit this shift (data not shown).

*Effect of  $\gamma_c$  Isoform on IP Synthase*

**Activity**—Purified  $\alpha$  isoform was obtained from Peak II fractions after Q-Sepharose chromatography (see “Experimental Procedures”). SDS-PAGE analysis confirmed that this enzyme lacked the  $\gamma_c$  isoform (Fig. 12, lane 1). The purified  $\alpha$  isoform was used in assays to determine the effect of recombinant  $\gamma_c$  isoform on IP synthase activity (Fig. 13). A profound decrease in  $\alpha$  isoform activity was observed in the presence of the  $\gamma_c$  isoform and  $\text{NAD}^+$  (Fig. 13, #3 versus #4 through #8). When the  $\gamma_c$  isoform was preincubated with  $\text{NAD}^+$ , prior to incubation with the  $\alpha$  isoform, the decrease was quite pronounced with enzyme activity falling to ~63% at the end of 1 h and to ~40% at the end of 3 h, after which no further decrease was seen (#3 versus #6–8). Without preincubation, the enzyme activity fell to a modest ~85% (#4 versus #3). To determine if interaction of the  $\gamma_c$  isoform with the  $\alpha$  isoform is a prerequisite for the observed decrease in activity, both isoforms were preincubated (for 1 h), prior to the addition of  $\text{NAD}^+$ . Little to no effect was observed (#4 versus #5). These results attribute the decrease in activity to competition by both isoforms for available  $\text{NAD}^+$  molecules. In these assays, bovine serum albumin (or IgG; not shown) was used as control, which showed no IP synthase activity (#1). The assays also clearly demonstrated the absolute requirement for  $\text{NAD}^+$  by the  $\alpha$  isoform (#2 versus #3) and that the  $\gamma_c$  isoform had no IP synthase activity (#9 versus #10). IP synthase activity of the control (#3) was relatively stable for the duration of the experiment (up to 16 h) with consistent  $A_{660}$  values.

**Molecular Weight of Various Isoforms**—We have generally used the apparent molecular mass of the various isoforms as determined by their migration on SDS-PAGE gels, e.g. the  $\alpha$  isoform migrates as a 68-kDa polypeptide, although its theoretical molecular mass is 61 kDa (Ref. 38, and this report). For isoforms that were first identified and characterized at the nucleic acid level (e.g.  $\beta$ ,  $\gamma_c$ ,  $\gamma_n$ ,  $\delta_c$ , and  $\delta_n$ ) the theoretical molecular mass has been used. Thus, the molecular mass of 16 kDa was assigned to the  $\gamma_c$  isoform, although it had an apparent

## myo-Inositol-3-phosphate Synthase Isoforms

**TABLE 1**

Mass spectrometry analysis of the 20-kDa polypeptide

Amino acid sequence of rat  $\gamma_c$  IP synthase:

... Exon 2 →  
**MEPAAEILVDS**PDVIFGPEAIEAR<sup>Y</sup>EYR<sup>T</sup>TRVSR**EGGVL**VRPTATRF<sup>T</sup>FR<sup>T</sup>TARQ  
 Exon 3 →  
 Exon 4 →  
**VR**RLGVMLV**GWGGN**NGSTLTAAVLANR**L**RLTW**P**TRTGRKEANY**Y**GS**L**TQAGTVNL  
 II III IV  
 Intron 4 →  
**GLDGDGR**EVFV**P**FSALL**P**MAPNDL**V**FDGG**Q**SLGM**G**WG.

Peptide	m/z Fragment <sup>a</sup>	[MH] <sup>+</sup> Matched <sup>b</sup>	Sequence of cleaved peptide <sup>c</sup>
I	800.4976	800.4743	(R)VRPTATRF
II	2371.1802	2371.2556	(R)LGVMLVWG <b>GGN</b> NGSTLTAAVLANR(L)
III	773.4636	773.4310	(R)LTWPTR(T)
IV	2371.1802	2371.1166	(K)EANY <b>Y</b> GS <b>L</b> TQAGTVNLGLDGDGR(E)

<sup>a</sup> Mass-to-charge ratio.

<sup>b</sup> Values for single charged ions.

<sup>c</sup> Identified peptides are underlined in the  $\gamma_c$  isoform amino acid sequence shown above; amino acids in parentheses: site of tryptic digestion.

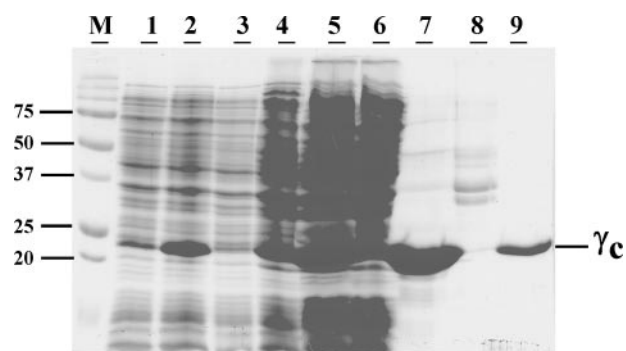


**FIGURE 10. Purification of bacterially expressed recombinant rat  $\gamma_c$  isoform.** An intact coding cDNA segment representing rat  $\gamma_c$  isoform was cloned into pRSET-A vector (with a 6 × His tag) and expressed in *E. coli* Rosetta (DE3) pLys cells. Proteins from various stages of purification were resolved on 12% SDS-PAGE and stained with Coomassie Blue. Lane M, molecular mass markers (kDa); lanes 1 and 2, extracts from uninduced and isopropyl 1-thio- $\beta$ -D-galactopyranoside induced cells (20  $\mu$ g of protein), respectively; lane 3, cell extract devoid of inclusion bodies (20  $\mu$ g of protein); lanes 4 and 5, inclusion bodies after detergent and water washes, respectively (40  $\mu$ g of protein); lane 6, urea insoluble pellet (40  $\mu$ g of protein); lane 7, inclusion bodies dissolved in 6 M urea buffer (20  $\mu$ g of protein); lane 8, unbound proteins from HisTrap column (5  $\mu$ g of protein); and lane 9, purified, refolded  $\gamma_c$  isoform (5  $\mu$ g of protein).

molecular mass of 20 kDa. Table 2 presents the molecular weights and salient features of the various isoforms described in this report.

## DISCUSSION

We identify for the first time the existence of various IP synthase isoforms at the nt and protein levels. These findings were triggered by the serendipitous discovery of a larger mRNA species that encodes a 16-kDa IP synthase polypeptide called the  $\gamma_c$  isoform. The  $\gamma_c$  isoform is of particular interest, because it is predominantly expressed in most tissues, along with the historically well studied 68-kDa protein (the  $\alpha$  isoform). Our findings disprove some widely held assumptions regarding mammalian IP synthase and raise exciting new questions about its role in inositol biosynthesis and regulation. Native IP synthase is not necessarily a 68-kDa homotrimer that is constitutively expressed in all (mammalian) tissues as is currently believed, but a far more complex entity that exists as a distinct holoen-

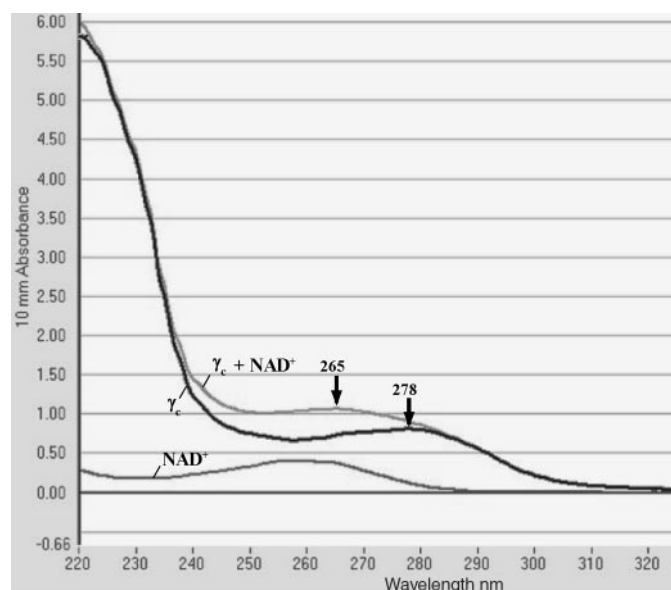


**FIGURE 11. UV absorption spectra of refolded recombinant  $\gamma_c$  isoform in the presence and absence of  $NAD^+$ .** Recombinant  $\gamma_c$  isoform after refolding, was used at a concentration of 1 mg/ml in the presence and absence of 20  $\mu$ M  $NAD^+$  in 50 mM Tris/HCl buffer, pH 8.0. A characteristic 'blue-shift' in the absorption maxima of the  $\gamma_c$  isoform from 278 to 265 nm occurs in the presence of  $NAD^+$ . This shift is not seen with the  $\gamma_c$  isoform denatured with 6 M Urea (not shown).

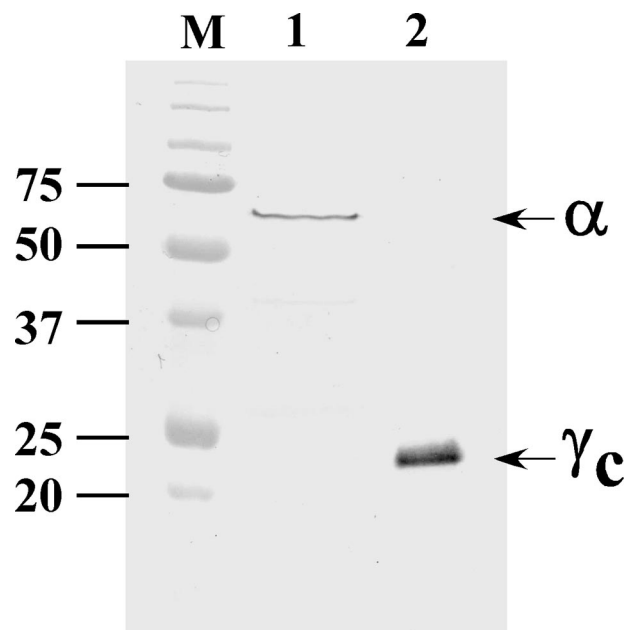


**FIGURE 12. Western blot analysis of purified rat testis  $\alpha$  and recombinant rat  $\gamma_c$  isoforms.** The purity of isoforms used for the determination of IP synthase activity is depicted. Lane 1, rat testis 68-kDa  $\alpha$  isoform partially purified from Peak II after Q-Sepharose chromatography (see "Experimental Procedures"). Note that this fraction does not contain native  $\gamma_c$  isoform. Lane 2, electrophoretically homogeneous recombinant rat  $\gamma_c$  isoform used to determine its effect on  $\alpha$  isoform enzyme activity. The rabbit polyclonal antibody R-10 was used to develop this immunoblot. M, protein molecular mass marker (in kDa).

zyme in different tissues, tailored, perhaps, to tissue-specific needs.

The existence of the  $\gamma_c$  isoform was confirmed by several criteria: (i) the identification of an intron 4-containing mRNA by PCR analysis and sequencing of cDNAs. That this transcript

is not an artifact is borne out by the fact that several partial rat mRNA sequences with intron 4 have been deposited in the NCBI database (see "Results"); additionally, intron 4-containing mRNAs are found to be conserved in other species such as mouse, Chinese hamster, and human; (ii) the highly conserved nature of the intron 4-encoded C-terminal peptide among rat, mouse, Chinese hamster, and human (Fig. 4B); the remarkably

high level of sequence conservation between Chinese hamster (a rodent) and human, two species that probably diverged ~70 million years ago (63), suggests a conserved functional role for this protein; (iii) the detection of a polypeptide with an apparent molecular mass of ~20 kDa, consistent with the size of the  $\gamma_c$  isoform, that remains tightly bound, in apparent stoichiometry, to the  $\alpha$  isoform in purified (testis) IP synthase preparations (Fig. 8); this finding is consistent with the detection of both isoforms by PCR analysis of testis cDNA (Fig. 6); (iv) the detection of a ~20-kDa polypeptide by a polyclonal antibody (R-10) raised against the  $\alpha$  isoform (Fig. 9); and (v) mass spectrometric analysis of tryptic digests of the ~20-kDa polypeptide (Table 1); four peptides matching the IP synthase sequence, all of them arising only from exons 2–4, a feature consistent with the presence of the  $\gamma_c$  isoform, were identified. These findings confirm the existence of the 16-kDa  $\gamma_c$  polypeptide as a novel IP synthase isoform with an apparent molecular mass of ~20 kDa.

The mRNA encoding the  $\gamma_c$  isoform is longer than that of the  $\alpha$  isoform because of read-through transcription of intron 4 where the gene segments "exon 4-intron 4-exon 5" constitute a single exonic unit. This novel mode of transcription (called intron retention or IR) generates two reading frames for translation, a short ORF encoding the 16-kDa  $\gamma_c$  isoform and a longer ORF encoding a 48-kDa  $\gamma_n$  isoform. The NCBI database expectedly identifies the  $\gamma_n$  polypeptide as the expressed protein (gene accession number BC079011), because the relatively larger size implies a higher probability of expression. But the  $\gamma_n$  isoform is not conserved in Chinese hamster and human implying a lack of viable function in mammalian tissues. On the contrary, the  $\gamma_c$  polypeptide is highly conserved among all four species studied (Fig. 4B). It is possible that the  $\gamma_n$  isoform is expressed only in mouse and rat, but this also seems unlikely because of the mechanistic dilemma posed by the mRNA to the translational machinery. For  $\gamma_n$  mRNA to be effectively translated into its cognate protein, the scanning mechanism would have to evade the first AUG in exon 2 before encountering the

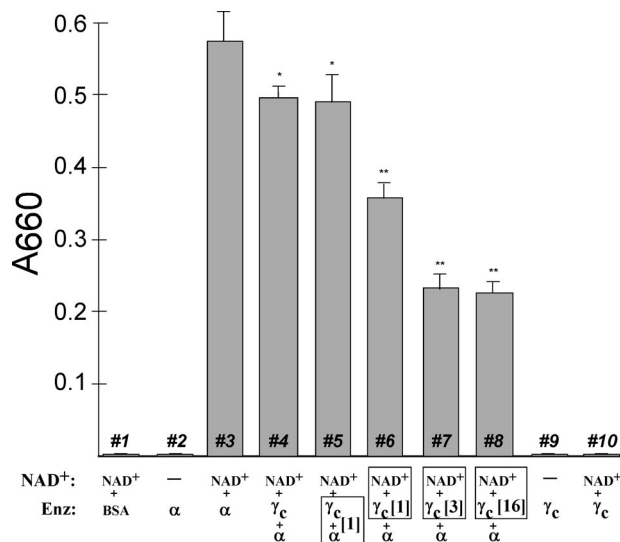


**FIGURE 13. Determination of the effect of the  $\gamma_c$  isoform on  $\alpha$  isoform activity.** IP synthase activity was measured as previously described (33). Samples (#1–10) were incubated either in the presence or absence of  $NAD^+$ , as shown at the bottom. Bovine serum albumin (or IgG, not shown) was used as a control. Partially purified rat testis  $\alpha$  isoform and purified bacterial recombinant rat  $\gamma_c$  isoform (see Fig. 12) were used for the assays. Reagents that were first preincubated are boxed with the time of preincubation (h) indicated within the box. Note that the  $\alpha$  isoform exhibits significant IP synthase activity only in the presence of  $NAD^+$  (#2 versus #3), whereas the  $\gamma_c$  isoform has no activity with  $NAD^+$  (#9 versus #10). Notably, the addition of the  $\gamma_c$  isoform to the  $\alpha$  isoform results in a significant decrease in activity (#3 versus #4–8). Experiments were done in triplicate and are indicated as Mean  $\pm$  S.D. All values were compared with that in #3 for calculating statistical significance, determined by one-way analysis of variance. \*,  $p < 0.05$ ; \*\*,  $p < 0.001$ .

**TABLE 2**  
Characterization of rat IP synthase isoforms

Isoform		Molecular mass <sup>a</sup>		Coding regions <sup>b</sup>	Tissue detected <sup>c</sup>	Detection		Comments	Refs.
		Calc.	App.			mRNA	Protein		
1.	$\alpha$	61	68	Ex 2–Ex 11	Most tissues; highest in testis	+	+	Historically well studied; present in most tissues; absent in intestine; fully spliced	This report (38, 42)
2.	$\beta$	59		Ex 2–Ex 11; deletion of 54bp at 3' of Ex 2	Testis, kidney	+	–	In-frame deletion of 18 aminoacids-A <sup>23</sup> to R <sup>40</sup> ; GC-AG splicing	This report
3.	$\gamma_c$	16	20	Ex 2–4 + Int 4	Testis, intestine, brain	+	+	Has $NAD^+$ domain, lacks catalytic domain; conserved in humans; novel C-terminus	This report
4.	$\gamma_n$	48		Int 4 + Ex 5–11		+	–	Not conserved in humans; lacks $NAD^+$ domain	This report
5.	$\delta_c$	14		Ex 2–3 + Int 3		–	–	Terminates in intron 3; novel C-terminus	GenBank <sup>TM</sup>
6.	$\delta_n$	48		Int 4 + Ex 5–11		–	–	Same as $\gamma_n$ ; possibly not expressed	GenBank <sup>TM</sup>
7.			66		Testis	–	+	Absent in pancreas, brain, intestine	This report
8.			62		Intestine	–	+	Absent in pancreas, brain, testes; lacks Ex 11	This report
9.			43		Intestine	–	+	Absent in pancreas, brain, testes	This report
10.			67		Pancreas	–	+	Absent in intestine, brain, testes	This report

<sup>a</sup> Calc., calculated; App., apparent.

<sup>b</sup> Ex: exon, Int: intron.

<sup>c</sup> Tissues are only those analyzed in this report.



## myo-Inositol-3-phosphate Synthase Isoforms

second in intron 4 (Fig. 3), which would violate Kozak's "first-AUG" rule (64). Re-initiation at the second AUG, after translation from the first, is also not possible because the second AUG is overlapped by the  $\gamma_c$  coding region (Fig. 5). Further, the nt sequence surrounding the first AUG (CTCGCCGCGAUGG) is in a highly favorable context for translation initiation having a 10/13 match (underlined) with the consensus initiation sequence, GCCGCCA/GCCAUGG, derived for vertebrate mRNAs, whereas the second AUG lies in a very poor sequence context, CGGGATGGGAUGG (6/13 match). No obstacles exist for  $\gamma_c$  mRNA translation, however, because initiation at the first AUG automatically terminates translation at an intron 4 stop codon. Although alternative mechanisms can be proposed for  $\gamma_n$  expression, it appears that the intron 4-transcribed mRNA expresses the  $\gamma_c$  isoform in mammalian tissues. Moreover, the lack of a NAD<sup>+</sup> binding domain in the  $\gamma_n$  isoform would also preclude this isoform from having any IP synthase activity; in contrast, even though the  $\gamma_c$  isoform lacks a catalytic domain, it has the capacity to bind NAD<sup>+</sup> and thereby modulate IP synthase activity (see below).

The  $\delta$  isoform was not detected in our cDNA analysis (*i.e.* no intron 3-containing cDNA was detected). For the  $\delta$  mRNA, both introns 3 and 4 are transcribed generating two putative isoforms (Fig. 3): (i) a 14-kDa  $\delta_c$  isoform encoded by an ORF that begins with the normal AUG codon in exon 2 and terminating in intron 3 and (ii) a 48-kDa  $\delta_n$  isoform identical to the  $\gamma_n$  isoform (note: an in-frame stop codon preceding the intron 4 AUG codon rules out any initiation upstream). The 14-kDa isoform bears all the hallmarks of expression, but the novel 29-amino acid intron 3-derived C-terminal peptide has little sequence resemblance to the cognate 60-amino acid human peptide (data not shown). The  $\delta$  mRNA can allow re-initiation to take place, because the two ORFs don't overlap, but the case for the expression of the 48-kDa isoform is still not compelling (as argued above). The 14-kDa  $\delta_c$  isoform is not the polypeptide detected in our analysis, because the mass spectrometric data identify an exon 4-derived peptide (Table 1) that is incompatible with the presence of this isoform. The failure to detect  $\delta_c$  mRNA in our samples could be due to its relatively low level of expression, to expression under certain conditions, or to the inability of the flanking PCR primers to amplify a relatively larger intron 3 segment (see Fig. 15).

IR transcripts have generally been considered to be the result of aberrant gene transcription associated with diseased states such as cancer, amyotrophic lateral sclerosis (65), *etc.* Such transcripts are usually targeted for degradation by the nonsense-mediated decay pathway. However, several recent findings now indicate that IR is an ancient and rare type of splicing mechanism that has evolved to generate genetic diversity (66, 67). Indeed, 15% of human genes encode IR transcripts that have significant biological relevance (68) and may explain, in part, why the human genome has an unusually low number of genes. Although some of these mRNAs regulate gene expression at the transcriptional level (69, 70), the rest function as expressed proteins (71–73). It would be interesting to find out how the  $\gamma_c$  mRNA evades the nonsense-mediated decay pathway. It is notable that the  $\gamma_c$  isoform lacks the catalytic domain present in the  $\alpha$  form and, hence, should display no IP synthase

activity (see below), but it harbors an NAD<sup>+</sup> binding site (Figs. 3 and 5) defined by the sequence GWGGNNG (amino acids 65–71 (Fig. 5)), which is reminiscent of the motif GXGXXG harbored by many Rossmann-fold NAD<sup>+</sup>-binding enzymes (40). Smaller isoforms can significantly affect the function of their parent isoforms as evidenced by the role truncated isoforms of transcription factors play in many cancers (74). Transcription factors harbor two domains, the DNA binding and activation domains, whereas truncated versions usually retain the former and, therefore, compete more efficiently for the DNA binding sites of the cognate transcription factor, thereby, regulating function negatively.

We determined the effects of the  $\gamma_c$  polypeptide on  $\alpha$  isoform activity using purified subunit preparations to see if it can negatively modulate enzyme activity (Fig. 13). First, consistent with the known properties of IP synthase, the  $\alpha$  isoform has an absolute requirement for NAD<sup>+</sup> for its activity. Second, as anticipated, the  $\gamma_c$  isoform has no IP synthase activity, even in the presence of NAD<sup>+</sup>, a property that can be attributed to the lack of the catalytic domain. This lack of activity was not due to misfolding of the bacterially expressed and purified  $\gamma_c$  polypeptide, because it was functionally capable of binding NAD<sup>+</sup>, as evidenced by a characteristic "blue shift" seen on UV absorption spectra analysis of the enzyme in the presence of NAD<sup>+</sup> (Fig. 11). In the presence of the  $\gamma_c$  isoform,  $\alpha$  isoform activity is significantly reduced, by up to 60%, when the  $\gamma_c$  isoform is first preincubated with NAD<sup>+</sup> (Fig. 13, #3 versus #7 and #8). Indeed, the decrease in activity appears to be proportional to the preincubation times: 0, 1, and 3 h (Fig. 13, #3 versus #4, #6, and #7). This decrease in activity is apparently not due to the  $\gamma_c$  isoform inducing conformational changes in the  $\alpha$  isoform, because preincubation of both isoforms prior to addition of NAD<sup>+</sup> did not change activity (Fig. 13, #4 versus #5). Presumably, preincubation of the  $\gamma_c$  isoform with NAD<sup>+</sup> depletes the intracellular NAD<sup>+</sup> pool resulting in less NAD<sup>+</sup> available for  $\alpha$  isoform activity. This is also borne out when the reaction is carried out with no preincubation where the decrease is a modest 15% (Fig. 13, #3 versus #4), possibly because the  $\alpha$  isoform can now compete with the  $\gamma_c$  isoform for an undepleted NAD<sup>+</sup> pool. More detailed kinetic analyses will be required to explain how the negative modulation of the  $\alpha$  isoform is effected. Determining the NAD<sup>+</sup> binding affinities of the two isoforms and determining the effect of different molar ratios of the isoforms on enzyme activity should be informative.

It has been assumed that native IP synthase exists as a trimer of the  $\alpha$  isoform ( $\alpha_3$ ) in most tissues, because this was the only polypeptide presumed to be expressed from the *Isyn1* gene. This assumption is no longer true, and we suggest a careful re-examination of IP synthase native structure in different tissues. Testis, a tissue that has long been well studied, harbors at least three isoforms: the  $\alpha$ ,  $\gamma_c$ , and a 66-kDa polypeptide. Indeed, the presence of the 68( $\alpha$ )- and 66-kDa subunits was probably observed as early as 1980 by Maeda and Eisenberg who concluded that "the intact enzyme is a trimer composed of at least two different subunits" (38). It is somewhat surprising that such an important property of IP synthase, which profoundly affects enzyme function and regulation, should have gone unnoticed all these years. In the intestine, a contrasting

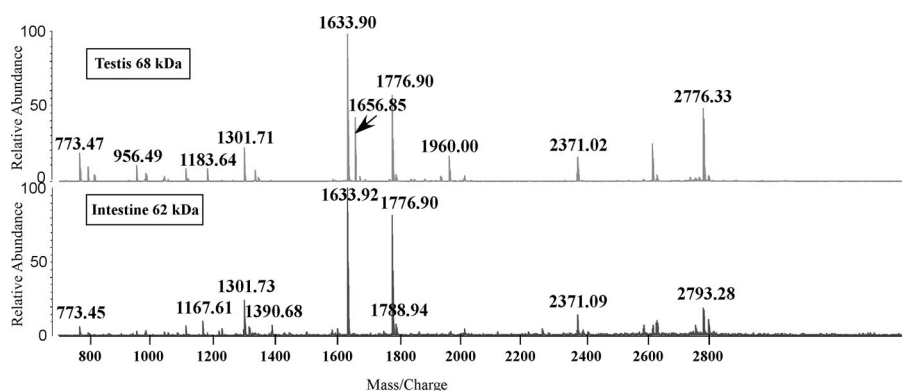


FIGURE 14. **Mass spectrometry analysis of the intestinal 62-kDa polypeptide.** MALDI-MS spectra of tryptic peptides from the intestinal 62-kDa (*lower panel*) isoform is compared with that derived from the 68-kDa  $\alpha$  isoform from testis (*upper panel*). The observed mass/charge ratio values for the tryptic fragments are indicated above each peak. All peptide fragments were identified using Mascot search. The most striking feature is the absence of the peptide at 1656.85 (arrow) in the intestine. This peptide corresponds to the sequence MERPF-PGIKPEEVK (residues 508–521) derived from exon 11.

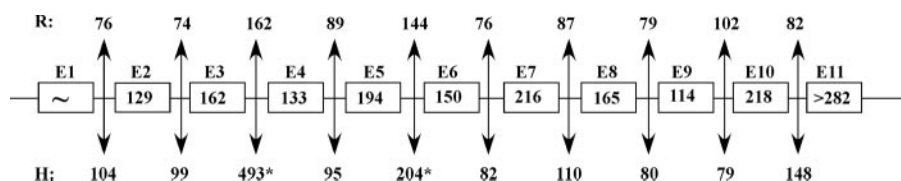


FIGURE 15. **Comparison of intron sizes between human and rat genes.** The 11 exons (E1–E11) for rat (*R*) and human (*H*) are shown. Exon sizes, indicated within the boxes, are common to both species, except for exon 1 whose size is not precisely known (~). Intron sizes are depicted above or below introns (double-headed arrows) for both species. Except for human introns 3 and 5 (asterisks), all introns are smaller than flanking exons. E11 is 282 bp in rat (gene accession number NM\_001013880) and 297–303 bp in human (gene accession numbers NM\_016369 and AF207640).

picture emerges with the  $\alpha$  isoform being notably absent (Fig. 9); rather, three new isoforms of 62, 43, and 16 ( $\gamma_c$ ) kDa are detected suggesting a completely different holoenzyme. The lack of the  $\alpha$  isoform in the intestine may not be surprising, because the intestine is apt to rely more on dietary sources and, therefore, on a more efficient transport system. However, this conclusion should await the characterization of the largest intestinal isoform: the 62-kDa protein. A MALDI-MS spectra comparison of the tryptic digests from the intestinal 62-kDa and the testicular 68-kDa polypeptides reveals the absence of peptides from exon 11 (Fig. 14), an observation confirmed by our inability to amplify an intact cDNA from exons 2–11 in this tissue (data not shown). The MS spectra indicate that the 62-kDa isoform is identical to the  $\alpha$  isoform from the N-terminal to at least residue Arg<sup>481</sup> (the last residue of the detected peptide in exon 10) or at best till residue Phe<sup>490</sup> (assuming exon 10 is completely translated); in any case, a novel C terminus must exist for this isoform. This feature is likely to alter the “central domain” responsible for making contacts between the monomers/subunits (see the introduction). The native molecular mass of rat and human brain enzymes has been determined to be 165 kDa (75), which cannot be accounted for solely by the presence of the  $\alpha$  isoform ( $\alpha_3$ : calculated and apparent molecular masses, 183 and 204 kDa, respectively). Our results indicate that this tissue harbors both the  $\gamma_c$  and  $\alpha$  isoforms predominantly, if not exclusively (Figs. 6 and 7A) suggesting that the native brain enzyme could putatively exist in an  $\alpha_2\gamma_c$  configuration (calculated and apparent molecular masses: 154 and 176 kDa, respectively), which is more in keeping with the

observed molecular mass. Our studies do not rule out the presence of additional undetected isoforms in brain, intestine, and testis enzymes.

Comparative differences in IP synthase mRNA expression are observed when rat tissues (this report) are compared with cognate human tissues (42). Although there is concordance in expression in testis (very high), spleen (low), and skeletal muscle (almost none), there are some significant differences with other tissues. In particular, the  $\gamma_c$  transcript, readily apparent on rat Northern blots, is not seen in human blots (42). This may be due to the high expression of human  $\alpha$  mRNA masking  $\gamma_c$  mRNA expression or to low expression of the latter in human tissues, as evidenced by our inability to amplify the  $\gamma_c$  mRNA with intron 4 flanking primers (amplifiable only with isoform-specific primers). These blots also indicate that, although the IP synthase mRNA is poorly expressed in human brain (42), it is relatively highly expressed in rat brain. Like-

wise, differences in mRNA expression are seen in rat *versus* human comparisons for kidney (high *versus* moderate), lung (high *versus* negligible), heart (moderate *versus* high), and liver (moderate *versus* low), respectively. Northern blots offer only a global picture of IP synthase expression; they do not discriminate between closely migrating isoforms or identify the specific isoform(s) being expressed. Indeed, the differences seen in rat *versus* human comparisons may be attributed to the expression of the individual isoforms in tissues. It is also not known if factors, such as tissue inositol levels, dictate the expression of any of these isoforms. For instance, is the  $\gamma_c$  isoform constitutively expressed or induced under certain conditions? This mRNA is expressed in fetal rats at 21 days of gestation suggesting a crucial role in early development. Indeed, inositol and folic acid are required during early development to significantly reduce neural tube defects in mice (76). Whether there is temporal regulation of any of these isoforms in any tissue remains to be carefully elucidated, and this is only possible if all isoforms are fully characterized at the protein and/or cDNA levels so that isoform-specific primers, probes, or antibodies could be utilized. For these reasons some of the PCR and Northern blot data presented here and in literature should be viewed with some caution. An intron 4-containing cDNA does not necessarily indicate the presence of the  $\gamma_c$  mRNA but could also suggest the  $\delta_c$  mRNA, which retains intron 4, or to other novel alternatively spliced isoform(s), hitherto uncharacterized, or to various combinations thereof.

The full repertoire of mammalian IP synthase isoforms is not known. We have identified at least seven rat isoforms at the RNA and protein levels (Table 2), while a preliminary analysis

## myo-Inositol-3-phosphate Synthase Isoforms

of human isoforms indicates the existence of at least 15 alternatively spliced transcripts (77) none of which has been characterized at the protein level. These isoforms appear to be generated by several mechanisms: IR ( $\gamma_c$  and  $\delta_c$  isoforms), in-frame deletions ( $\beta$  isoform), exon skipping (59, 77), partial IR (77), splicing within exons (77), etc., with a majority of human transcripts showing IR (7/15) and exon skipping (5/15). IR is presumed to occur because of the failure to recognize weak splice sites flanking short introns by the "intron definition" mechanism. Mammalian genes typically have short exons interspersed by large introns, a feature that appears to facilitate splice-site recognition through the "exon definition" model (78), which is not the case for rat *Isyna1* where almost all introns are found to be smaller than exons: mean size of 97 bp versus 177 bp, respectively (Fig. 15). Indeed, with the possible exception of intron 1, no introns are larger than the flanking exons. This is also true for the human *ISYNA1* gene (Fig. 15) where all introns, except 3 (493 bp) and 5 (204 bp), are smaller than (flanking) exons. Clearly, the rat and human genes have unique structures primed for generating multiple mRNAs.

Our observations have a profound impact in understanding inositol homeostasis in mammalian cells and pose several interesting questions. The presence of several IP synthase isoforms, both in rats and humans, suggests that inositol biosynthesis by IP synthase is a highly regulated and complex process. A major task would be to unravel the function of each of these isoforms and determine how they affect IP synthase activity. This is necessary for the proper understanding of inositol homeostasis in various cell types, the action of various psychoactive drugs that have been examined primarily in the context of the  $\alpha$  isoform, and in interpreting phenotypic effects of mutations. The identification of isoforms also increases the chance of disease-causing mutations, because defects can now be attributed to isoform deficiency caused by aberrant splicing.

*Acknowledgment*—We are indebted to members of the Radiology Service, Veterans Affairs Medical Center, Louisville, KY, for permission to use their X-ray facilities.

## REFERENCES

1. Parthasarathy, L. K., Seelan, R. S., Tobias, C., Casanova, M. F., and Parthasarathy, R. N. (2006) *Subcell. Biochem.* **39**, 293–314
2. Irvine, R. F., and Schell, M. J. (2001) *Nat. Rev. Mol. Cell Biol.* **2**, 327–338
3. Berridge, M. J., Lipp, P., and Bootman, M. D. (2000) *Science* **287**, 1604–1605
4. Saiardi, A., Bhandari, R., Resnick, A. C., Snowman, A. M., and Snyder, S. H. (2004) *Science* **306**, 2101–2105
5. Shen, X., Xiao, H., Ranallo, R., Wu, W. H., and Wu, C. (2003) *Science* **299**, 112–114
6. Steger, D. J., Haswell, E. S., Miller, A. L., Wenthe, S. R., and O'Shea, E. K. (2003) *Science* **299**, 114–116
7. Odom, A. R., Stahlberg, A., Wenthe, S. R., and York, J. D. (2000) *Science* **287**, 2026–2029
8. York, J. D., Odom, A. R., Murphy, R., Ives, E. B., and Wenthe, S. R. (1999) *Science* **285**, 96–100
9. Vaden, D. L., Ding, D., Peterson, B., and Greenberg, M. L. (2001) *J. Biol. Chem.* **276**, 15466–15471
10. Williams, R. S. B., Cheng, L., Mudge, A. W., and Harwood, A. J. (2002) *Nature* **417**, 292–295
11. Wong, Y. H., Kalmbach, S. J., Hartman, B. K., and Sherman, W. R. (1987) *J. Neurochem.* **48**, 1434–1442
12. Harwood, A. J. (2005) *Mol. Psychiatry* **10**, 117–126
13. Delmas, P., Coste, B., Gamper, N., and Shapiro, M. S. (2005) *Neuron* **47**, 179–182
14. Berridge, M. J. (1993) *Nature* **361**, 315–325
15. Lee, S. B., and Rhee, S. G. (1995) *Curr. Opin. Cell Biol.* **7**, 183–189
16. McLaurin, J., Franklin, T., Chakrabarty, A., and Fraser, P. E. (1998) *J. Mol. Biol.* **278**, 183–194
17. Shimohama, S., Tanino, H., Sumida, Y., Tsuda, J., and Fujimoto, S. (1998) *Neurosci. Lett.* **245**, 159–162
18. Friedman, S. D., Shaw, D. W., Artru, A. A., Richards, T. L., Gardner, J., Dawson, G., Posse, S., and Dager, S. R. (2003) *Neurology* **60**, 100–107
19. Shimon, H., Agam, G., Belmaker, R. H., Hyde, T. M., and Kleinman, J. E. (1997) *Am. J. Psychiatry* **154**, 1148–1150
20. Rumpel, H., Lim, W. E., Chang, H. M., Chan, L. L., Ho, G. L., Wong, M. C., and Tan, K. P. (2003) *J. Magn. Reson. Imaging* **17**, 11–19
21. Macri, M., D'Alessandro, N., Di Giulio, C., Di Iorio, P., Di Luzio, S., Giuliani, P., Bianchi, G., and Esposito, E. (2006) *Neurobiol. Aging* **27**, 98–104
22. Berry, G. T., Mallee, J. J., Kwon, H. M., Rim, J. S., Mulla, W. R., Muenke, M., and Spinner, N. B. (1995) *Genomics* **25**, 507–513
23. Acevedo, L. D., Holloway, H. W., Rapoport, S. I., and Shetty, H. U. (1997) *J. Mass Spectrom.* **32**, 395–400
24. Cockroft, D. L. (1988) *Teratology* **38**, 281–290
25. Harvey, B. H., Brink, C. B., Seedat, S., and Stein, D. J. (2002) *Prog. Neuropsychopharmacol. Biol. Psychiatry* **26**, 21–32
26. Fux, M., Levine, J., Aviv, A., and Belmaker, R. H. (1996) *Am. J. Psychiatry* **153**, 1219–1221
27. Benjamin, J., Levine, J., Fux, M., Aviv, A., Levy, D., and Belmaker, R. H. (1995) *Am. J. Psychiatry* **152**, 1084–1086
28. Silver, S. M., Schroeder, B. M., Sterns, R. H., and Rojiani, A. M. (2006) *J. Neuropathol. Exp. Neurol.* **65**, 37–44
29. Einat, H., and Belmaker, R. H. (2001) *J. Affect. Disord.* **62**, 113–121
30. Levine, J., Barak, Y., Gonzalves, M., Szor, H., Elizur, A., Kofman, O., and Belmaker, R. H. (1995) *Am. J. Psychiatry* **152**, 792–794
31. Ju, S., and Greenberg, M. L. (2004) *Clin. Neurosci. Res.* **4**, 181–187
32. Agam, G., Shamir, A., Shaltiel, G., and Greenberg, M. L. (2002) *Bipolar Disord.* **4**, Suppl. 1, 15–20
33. Eisenberg, F., Jr., and Parthasarathy, R. (1987) *Methods Enzymol.* **141**, 127–143
34. Loewus, F. A., and Kelly, S. (1962) *Biochem. Biophys. Res. Commun.* **7**, 204–208
35. Eisenberg, F., Jr. (1967) *J. Biol. Chem.* **242**, 1375–1382
36. Eisenberg, F., Jr., Bolden, A. H., and Loewus, F. A. (1964) *Biochem. Biophys. Res. Commun.* **14**, 419–424
37. Kindl, H., and Hoffmann-Ostenhof, O. (1964) *Biochem. Z.* **339**, 374–381
38. Maeda, T., and Eisenberg, F., Jr. (1980) *J. Biol. Chem.* **255**, 8458–8464
39. Majumder, A. L., Chatterjee, A., Dastidar, K. G., and Majee, M. (2003) *FEBS Lett.* **553**, 3–10
40. Stein, A. J., and Geiger, J. H. (2002) *J. Biol. Chem.* **277**, 9484–9491
41. Jin, X., Foley, K. M., and Geiger, J. H. (2004) *J. Biol. Chem.* **279**, 13889–13895
42. Guan, G., Dai, P., and Shechter, I. (2003) *Arch. Biochem. Biophys.* **417**, 251–259
43. McCauley, J. L., Li, C., Jiang, L., Olson, L. M., Crockett, G., Gainer, K., Folstein, S. E., Haines, J. L., and Sutcliffe, J. S. (2005) *BMC Med. Genet.* **6**, 1
44. Greenberg, M. L., and Lopes, J. M. (1996) *Microbiol. Rev.* **60**, 1–20
45. Carman, G. M., and Henry, S. A. (1999) *Prog. Lipid Res.* **38**, 361–399
46. Culbertson, M. R., Donahue, T. F., and Henry, S. A. (1976) *J. Bacteriol.* **126**, 232–242
47. Klig, L. S., and Henry, S. A. (1984) *Proc. Natl. Acad. Sci. U. S. A.* **81**, 3816–3820
48. Hirsch, J. P., and Henry, S. A. (1986) *Mol. Cell. Biol.* **6**, 3320–3328
49. Ju, S., Shaltiel, G., Shamir, A., Agam, G., and Greenberg, M. L. (2004) *J. Biol. Chem.* **279**, 21759–21765
50. Berridge, M. J., Downes, C. P., and Hanley, M. R. (1989) *Cell* **59**, 411–419
51. Berry, G. T., Buccafusca, R., Greer, J. J., and Eccleston, E. (2004) *Mol. Genet. Metab.* **82**, 87–92
52. Whiting, P. H., Palmano, K. P., and Hawthorne, J. N. (1979) *Biochem. J.*



- 179, 549–553
53. Hasegawa, R., and Eisenberg, F., Jr. (1981) *Proc. Natl. Acad. Sci. U. S. A.* **78**, 4863–4866
  54. Rivera-Gonzalez, R., Petersen, D. N., Tkalcevic, G., Thompson, D. D., and Brown, T. A. (1998) *J. Steroid Biochem. Mol. Biol.* **64**, 13–24
  55. Naccarato, W. F., Ray, R. E., and Wells, W. W. (1974) *Arch. Biochem. Biophys.* **164**, 194–201
  56. Shamir, A., Shaltiel, G., Greenberg, M. L., Belmaker, R. H., and Agam, G. (2003) *Brain Res. Mol. Brain Res.* **115**, 104–110
  57. Seelan, R. S., Parthasarathy, L. K., and Parthasarathy, R. (2004) *Arch. Biochem. Biophys.* **431**, 95–106
  58. Strausberg, R. L., Feingold, E. A., Grouse, L. H., Derge, J. G., Klausner, R. D., Collins, F. S., Wagner, L., Shenmen, C. M., Schuler, G. D., Altschul, S. F., Zeeberg, B., Buetow, K. H., Schaefer, C. F., Bhat, N. K., Hopkins, R. F., Jordan, H., Moore, T., Max, S. I., Wang, J., Hsieh, F., Diatchenko, L., Marusina, K., Farmer, A. A., Rubin, G. M., Hong, L., Stapleton, M., Soares, M. B., Bonaldo, M. F., Casavant, T. L., Scheetz, T. E., Brownstein, M. J., Usdin, T. B., Toshiyuki, S., Carninci, P., Prange, C., Raha, S. S., Loquellano, N. A., Peters, G. J., Abramson, R. D., Mullahy, S. J., Bosak, S. A., McEwan, P. J., McKernan, K. J., Malek, J. A., Gunaratne, P. H., Richards, S., Worley, K. C., Hale, S., Garcia, A. M., Gay, L. J., Hulyk, S. W., Villalon, D. K., Muzny, D. M., Sodergren, E. J., Lu, X., Gibbs, R. A., Fahey, J., Helton, E., Kettelman, M., Madan, A., Rodrigues, S., Sanchez, A., Whiting, M., Madan, A., Young, A. C., Shevchenko, Y., Bouffard, G. G., Blakesley, R. W., Touchman, J. W., Green, E. D., Dickson, M. C., Rodriguez, A. C., Grimwood, J., Schmutz, J., Myers, R. M., Butterfield, Y. S., Krzywinski, M. I., Skalska, U., Smailus, D. E., Schnerch, A., Schein, J. E., Jones, S. J., and Marra, M. A. (Mammalian Gene Collection Program Team) (2002) *Proc. Natl. Acad. Sci. U. S. A.* **99**, 16899–16903
  59. Shamir, A., Shaltiel, G., Mark, S., Bersudsky, Y., Belmaker, R. H., and Agam, G. (2007) *Bipolar Disord.* **9**, 766–771
  60. Chen, J., He, L., Dinger, B., Stensaas, L., and Fidone, S. (2002) *J. Appl. Physiol.* **92**, 1480–1486
  61. Jensen, O. N., Wilm, M., Shevchenko, A., and Mann, M. (1999) *Methods Mol. Biol.* **112**, 513–530
  62. Malhotra, O. P., and Bernhard, S. A. (1973) *Proc. Natl. Acad. Sci. U. S. A.* **70**, 2077–2081
  63. Douzery, E. J., Delsuc, F., Stanhope, M. J., and Huchon, D. (2003) *J. Mol. Evol.* **57**, Suppl. 1, S201–S213
  64. Kozak, M. (1989) *J. Cell Biol.* **108**, 229–241
  65. Xiao, S., Tjostheim, S., Sanelli, T., McLean, J. R., Horne, P., Fan, Y., Ravits, J., Strong, M. J., and Robertson, J. (2008) *J. Neurosci.* **28**, 1833–1840
  66. Sakabe, N. J., and de Souza, S. J. (2007) *BMC Genomics* **8**, 59
  67. Kim, E., Magen, A., and Ast, G. (2007) *Nucleic Acids Res.* **35**, 125–131
  68. Galante, P. A., Sakabe, N. J., Kirschbaum-Slager, N., and de Souza, S. J. (2004) *RNA* **10**, 757–765
  69. Xu, Q., Walker, D., Bernardo, A., Brodbeck, J., Balestra, M. E., and Huang, Y. (2008) *J. Neurosci.* **28**, 1452–1459
  70. Mansilla, A., Lopez-Sanchez, C., de la Rosa, E. J., Garcia-Martinez, V., Martinez-Salas, E., de Pablo, F., and Hernandez-Sanchez, C. (2005) *EMBO Rep.* **6**, 1182–1187
  71. Blanco, E., Rojas, R., Haeger, P., Cuevas, R., Perez, C., Munita, R., Quiroz, G., Andres, M. E., Forray, M. I., and Gysling, K. (2006) *Neuroscience* **140**, 1245–1252
  72. Auffray, C., Gayon, R., Benraiss, A., Martin, N., Laurendeau, I., Garaud, J., Lucas, B., Boitard, C., and Krief, P. (2006) *Exp. Cell Res.* **312**, 233–244
  73. Melhuish, T. A., and Wotton, D. (2006) *BMC Mol. Biol.* **7**, 2
  74. DeYoung, M. P., and Ellisen, L. W. (2007) *Oncogene* **26**, 5169–5183
  75. Adhikari, J., and Majumder, A. L. (1988) *Indian J. Biochem. Biophys.* **25**, 408–412
  76. Greene, N. D. E., and Copp, A. J. (1997) *Nat. Med.* **3**, 60–66
  77. Stamm, S., Riethoven, J.-J., Le Texier, V., Gopalakrishnan, C., Kumanduri, V., Tang, Y., Barbosa-Morais, N. L., and Thanaraj, T. A. (2006) *Nucleic Acids Res.* **34**, D46–D55
  78. Berget, S. M. (1995) *J. Biol. Chem.* **270**, 2411–2414